Dissertation

Investigations on the role of translation initiation factors in aggressive B-cell lymphoma

submitted by

Julia Judith UNTERLUGGAUER,

BSc MSc

for the Academic Degree of

Doctor of Philosophy

(PhD)

at the

Medical University of Graz

Diagnostic and Research Institute of Pathology

under the Supervision of

Univ.- Prof. Dr.med.univ. Dr.sc.nat. Johannes HAYBÄCK

2018

Statutory Declaration

I hereby declare that this thesis is my own original work and that I have fully acknowledged by name all of those individuals and organisations that have contributed to the research for this thesis. Due acknowledgement has been made in the text to all other material used. Throughout this thesis and in all related publications I followed the “Standards of Good Scientific Practice and Ombuds Committee at the Medical University of Graz”.

Graz, December 2018

Disclosures

Part of this thesis has been published in

Blood Cancer Journal. 2018;8:79.

Expression profile of translation initiation factor eIF2B5 in diffuse large B-cell lymphoma and its correlation to clinical outcome

Julia J. Unterluggauer[1], Katharina Prochazka[2], Peter V. Tomazic[3], Heinrich J. Huber[4], Rita Seeboeck[5], Karoline Fechter[2], Elisabeth Steinbauer[1], Verena Gruber[1], Julia Feichtinger[6,7], Martin Pichler[8], Marc A. Weniger[9], Ralf Küppers[9,10], Heinz Sill[2], Rudolf Schicho[11], Peter Neumeister[2], Christine Beham-Schmid[1], Alexander J. A. Deutsch[2*], and Johannes Haybaeck[1,12*]

**These authors contributed equally to this work.*

[1]Diagnostic and Research Institute of Pathology, Diagnostic and Research Center for Molecular BioMedicine, Medical University of Graz, Graz, Austria

[2]Division of Hematology, Medical University of Graz, Graz, Austria

[3]Department of Otorhinolaryngology, Medical University of Graz, Graz, Austria

[4]Institute for Automation Engineering, Otto von Guericke University Magdeburg, Magdeburg, Germany

[5]Department Life Sciences, IMC University of Applied Sciences Krems, Krems, Austria

[6]Institute of Computational Biotechnology, Graz University of Technology, Graz, Austria

[7]BioTechMed Omics Center Graz, Graz, Austria

[8]Department of Internal Medicine, Medical University of Graz, Graz, Austria

[9]Institute of Cell Biology (Cancer Research), University of Duisburg-Essen, Essen, Germany

[10]German Cancer Consortium (DKTK), Heidelberg, Germany

[11]Division of Pharmacology, Otto Loewi Research Center, Medical University of Graz, Graz, Austria

[12]Department of Pathology, Medical Faculty, Otto von Guericke University Magdeburg, Magdeburg, Germany

All co-authors agreed to the use of their data in the thesis. Reproduction/adaptation of figures and tables has been permitted by the Creative Commons Attribution 4.0 International License of the article. Permission to reproduce respective other figures in the dissertation has been obtained (see respective sections).

Contributions of co-authors to the thesis and the respective publication:

Katharina Prochazka collected the clinical data of the study cohort.

Peter V. Tomazic gathered non-neoplastic tissue, used in immunohistochemical and mRNA analysis, in course of tonsillectomies and informed the respective patients.

Heinrich J. Huber and Martin Pichler helped in calculating the multivariate analysis.

Rita Seeboeck, Heinz Sill, Rudolf Schicho and Peter Neumeister gave input in project design.

Karoline Fechter supported the preparation of patient samples.

Elisabeth Steinbauer and Verena Gruber performed the immunohistochemical stainings used in the study.

Julia Feichtinger prepared the two external patient cohorts for survival analysis.

Marc A. Weniger and Ralf Küppers isolated the germinal center B-cells for mRNA expression analysis.

Christine Beham-Schmid established the study cohort and supported immunohistochemical analysis.

Alexander J. A. Deutsch co-supervised the project, established the study cohort, and critically helped in all steps of study performance.

Johannes Haybaeck supervised the project.

To

Maria Pansi

1929 – 2015

Acknowledgements

At this point, I would like to express my gratitude to all those, without whom this dissertation would not have been possible.

I would like to thank my supervisor Prof. Johannes Haybäck for giving me the opportunity to realize this work. Thank you for choosing this topic for me that I really enjoyed working on and thank you also for your very positive and friendly way, which always motivated me! I would like to thank also my lab mates at the Haybäck lab, with whom I spent a precious time that I would not want to miss.

I am deeply thankful to Priv.-Doz. Alexander Deutsch, who supported me in every possible way. You gave me priceless scientific and personal advice! Thank you for being there for me! Also big thanks to the Deutsch lab, who always made me feel very welcome. I had a great time with all of you!

I would like to express my gratitude to all the co-authors of my paper in “Blood Cancer Journal”. Thank you all for the good collaboration and for your support in realizing this project!

I would like to thank the Medical University of Graz, from which I received funding through the PhD Program “Molecular Medicine” (Mol Med). In this context, I would also like to thank for the good organization of the PhD program. Moreover, I am grateful for all the advice, I received from my thesis committee, including Prof. Heinz Sill und Assoz. Prof. Rudolf Schicho.

Mille grazie anche a Dr. Luca Abete, un carissimo italiano in Austria!

Finally, I come to my family and friends. The time of my PhD was not always an easy one and without all of you, I would not have made it! I am so grateful to my parents for supporting me not only throughout this PhD but throughout my entire life. You are always there to raise me up and bring me back on the track! Last but not least, I would like to thank Florian, who came into my life during this PhD and brought with him a lot of sunshine. Thank you for your love and motivation that held me up!

Table of Contents

Abbreviations and Definitions

4E-BP1	eIF4E-binding protein 1
5´ UTR	5´ untranslated region
A20/TNFAIP3	tumor necrosis factor α-induced protein 3
ABC	activated B-like DLBCL
Ago2	protein argonaute-2
AID	activation-induced cytidine deaminase
ATP	adenosine triphosphate
B2M	β2 microglobulin
BCL-2	B-cell CLL/lymphoma 2
BCL-6	B-cell CLL/lymphoma 6
BCR	B-cell receptor
Blimp-1	B lymphocyte–induced maturation protein-1
BTK	Bruton tyrosine kinase
CARD11	caspase recruitment domain-containing protein 11
CD	cluster of differentiation
cDNA	complementary deoxyribonucleic acid
CHOP	cyclophosphamide, doxorubicin, vincristine, and prednisone
CREBBP	CREB binding protein
CSR	class switch recombination
CT	computed tomography
DAP5	death associated protein 5
DH/TH	double- and triple-hit
DLBCL	diffuse large B-cell lymphoma
DMEM	Dulbecco's Modified Eagle Medium
DPBS	Dulbecco's phosphate-buffered saline
DTT	dithiothreitol
EDTA	ethylenediaminetetraacetic acid

eIF	eukaryotic initiation factor
EP300	E1A binding protein p300
ER	endoplasmic reticulum
EZH2	enhancer of zeste homolog 2
FASN	fatty acid synthase
FDC	follicular dendritic cell
FL	follicular lymphoma
FOXO1	forkhead box protein O1
GAP	GTPase accelerating protein
GC	germinal center
GCB	germinal center B-like DLBCL
GDI	GDP dissociation inhibitor
GDP	guanosine diphosphate
GEF	guanine nucleotide exchange factor
GNA13 / Gα13	guanine nucleotide binding protein alpha 13
GTP	guanosine triphosphate
Hsp90	heat shock protein 90
Ig	immunoglobulin
IHC	immunohistochemistry
IMDM	Iscove's Modified Dulbecco's Medium
IPI	International Prognostic Index
MCL-1	myeloid cell leukemia-1
Met-tRNA$_i$	methionyl-tRNA
MHC	major histocompatibility complex
miRNA	microRNA
MNK	mitogen-activated protein kinase interacting kinase
mRNA	messenger RNA
mRNP	messenger ribonucleoprotein
mTOR	mammalian target of rapamycin
MUM1	multiple myeloma oncogene 1

MyD88	myeloid differentiation primary response 88
na	not applicable
NF-κB	nuclear factor kappa B
nGCB-DLBCL	non-GCB-DLBCL
NHL	non-Hodgkin lymphoma
NK-cell	natural killer-cell
Notch 1	neurogenic locus notch homolog protein 1
Notch 2	neurogenic locus notch homolog protein 2
p	phospho
PET	positron emission tomography
pGCB	primary GCB-DLBCL
PI3K	phosphoinositide 3-kinase
PIC	pre-initiation complex
PVDF	polyvinylidene difluoride
qRT-PCR	quantitative real-time PCR
RAG1	recombination activating gene 1
RAG2	recombination activating gene 2
R-CHOP	CHOP plus rituximab
RNA	ribonucleic acid
SDS	sodium dodecyl sulfate
SDS-PAGE	sodium dodecyl sulfate–polyacrylamide gel electrophoresis
sGCB	secondary GCB-DLBCL originating from an FL grade 3
SHM	somatic hypermutation
siRNA	small interfering RNA
TBS	tris-buffered saline
tRNA	transfer RNA
UPR	unfolded protein response
USP11	ubiquitin-specific protease 11

List of Figures

List of Tables

Abstract in German

Das diffus großzellige B-Zell-Lymphom (DLBCL) ist eine aggressive neoplastische Erkrankung, die das lymphatische System betrifft. Obwohl eine zeitgemäße Chemo-Immuntherapie einen nicht unerheblichen Teil der DLBCL-Patient/innen heilen kann, sterben dennoch 40% der Betroffenen an ihrer Erkrankung. Ein Grund hierfür liegt in der großen Heterogenität der Neoplasie, welche sich unter anderem in zwei krankheitsrelevanten Subtypen widerspiegelt. Um von dieser heterogenen Erkrankung betroffenen Patient/innen helfen zu können, besteht daher ein ständiger Bedarf an neuen diagnostischen oder prognostischen Markern, um das Risiko der Betroffenen *a priori* feststellen und um darüber hinaus auch neue zielgerichtete Therapien ermöglichen zu können.

Die zelluläre Proteinsynthese beginnt mit der Stufe der Translations-Initiation. Diese stellt eine wichtige Regulationsstufe des gesamten Prozesses dar. Die Funktion der Translations-Initiation, die durch sogenannte eukaryontische Translations-Initiationsfaktoren (eIFs) realisiert wird, besteht darin, ein Elongations-kompetentes Ribosom auf der Protein-kodierenden mRNA zusammenzubauen. Neben dieser entscheidenden Rolle im regulären Zellmetabolismus weiß man heute aber auch, dass eIFs zu verschiedenen neoplastischen Erkrankungen beitragen. Beim DLBCL wurden, abgesehen von bestimmten eIFs, die bereits mit seiner Pathogenese in Zusammenhang gebracht wurden, die meisten eIFs jedoch noch nie untersucht.

Um diese Lücke zu schließen und zugleich nach neuen Markern für die DLBCL-Pathogenese zu suchen, wurden in dieser Studie 16 eIFs auf ihre mögliche krankheitsrelevante Rolle im DLBCL hin analysiert. Zu diesem Zweck wurde bei einer Kohorte, bestehend aus primären (n=34) und sekundären (n=22) DLBCL-Patientenproben, die mRNA-Expression des untersuchten eIF-Panels bestimmt. Als nicht neoplastische Kontrollen wurden Keimzentrums-B-Zellen eingeschlossen, welche aus nicht neoplastischen Tonsillen (n=5) isoliert wurden. Die Auswertung zeigte eine höhere Expression von 12 der 16 eIFs im DLBCL im Vergleich zu den nicht neoplastischen B-Zell-Kontrollen ($p<0,003$). Weiters wiesen 8 eIFs des untersuchten Panels eine höhere mRNA-Expression im aggressiveren

im Vergleich zum weniger aggressiven DLBCL-Subtyp auf ($p<0,05$). Anschließende immunhistochemische und Westernblot-Untersuchungen auf Proteinebene bestätigten die Überexpression von eIF1A und eIF3d im DLBCL. Im Fall von eIF2B5 zeigten die mRNA-Daten nicht nur eine Überexpression im DLBCL auf, sondern auch eine Assoziation mit dem aggressiveren der beiden DLBCL-Subtypen. Beides konnte mittels immunhistochemischer Analyse bestätigt werden ($p<0,04$). Des Weiteren ergab die Auswertung auch eine Assoziation zwischen hoher *EIF2B5* mRNA-Expression und schlechterem Patientenüberleben in der Studienkohorte ($p=0,005$). Dieses Resultat konnte in zwei öffentlich zugänglichen Expressions-Datensätzen von DLBCL-Patient/innen ($n=58$ und $n=200$, $p<0,015$) und auch auf Proteinebene mittels Immunhistochemie ($p=0,006$) bestätigt werden. Schließlich stellte sich *EIF2B5* in der multivariaten Analyse auch als unabhängiger prognostischer Faktor im DLBCL heraus ($p=0,003$).

Zusammenfassend zeigte die hier vorgestellte Studie einen stark deregulierten Translations-Initiationsweg im DLBCL auf. Besonders hervorzuheben sind jedoch die Ergebnisse von eIF2B5, welche auf ein mögliches prognostisches und diagnostisches Potenzial dieses eIFs in der DLBCL-Pathogenese hinweisen.

Abstract in English

Diffuse large B-cell lymphoma (DLBCL) is an aggressive neoplasm affecting the lymphatic system. Although contemporary chemo-immunotherapy can cure a considerable fraction of DLBCL-patients, 40% still succumb to their disease. Importantly, one reason for this lies in the big heterogeneity of the malignancy, which is reflected, amongst others, by two disease-relevant subtypes. In order to help patients affected by this heterogeneous disease, there is thus a constant need for new diagnostic or prognostic markers, to be able to stratify patients risk *a priori* and to enable moreover new targeted therapies.

Cellular protein synthesis begins with the translation initiation phase, a key control step of the whole process. The task of translation initiation, which is realized by so-called eukaryotic initiation factors (eIFs), is to assemble an elongation-competent ribosome on the protein-coding mRNA. Importantly, despite this crucial role in regular cell metabolism, eIFs have also been described to contribute to diverse neoplastic settings. Nevertheless, apart from specific eIFs having already been implicated in DLBCL pathogenesis, most eIFs have never been investigated in this malignancy.

To fill this gap and to look for new markers for DLBCL pathogenesis, in this study, 16 eIFs were investigated for their potential disease-relevant role in DLBCL. For this aim, a cohort of primary (n=34) and secondary (n=22) DLBCL patient samples was analyzed for the mRNA expression levels of the investigated eIF-panel. As non-neoplastic controls, germinal center B-cell specimens, isolated from non-neoplastic tonsils (n=5), were used. Interestingly, 12 out of 16 eIFs were higher expressed in DLBCL than in non-neoplastic B-cell controls ($p<0.003$). Furthermore, 8 eIFs of the investigated panel showed higher mRNA expression in the more aggressive DLBCL subtype when compared to the less aggressive one ($p<0.05$). Subsequent investigation on the protein level confirmed overexpression of eIF1A and eIF3d in DLBCL by immunohistochemical and Western blot analysis. For *EIF2B5*, the mRNA data revealed not only overexpression in DLBCL, but also an association with the more aggressive DLBCL subtype, which could be both confirmed by immunohistochemical analysis ($p<0.04$). Interestingly, high *EIF2B5*

mRNA expression was moreover detected to be associated with worse patient outcome in the study cohort (p=0.005), a finding that could be confirmed in two publicly available expression data sets of DLBCL patients (n=58 and n=200, p<0.015) and also on the protein level using immunohistochemical stainings (p=0.006). Finally, multivariate analysis revealed *EIF2B5* as independent prognostic factor in DLBCL (p=0.003).

To sum up, the present study uncovered a heavily dysregulated translation initiation pathway in DLBCL. Especially remarkable were, however, the results for eIF2B5, which indicate possible prognostic and diagnostic utility of this eIF in DLBCL pathogenesis.

1 Introduction

1.1 Lymphoma

1.1.1 Lymphoma – a heterogenous disease

Lymphoma refers to a group of various neoplasms that affect the lymphatic system (1). In Austria, out of 100,000 people, about 20 new cases of lymphoma are diagnosed annually (2-4). The malignant tumors often start in the lymphatic system, e.g. in lymph nodes, from where they can spread to other parts of the human body, such as the liver or lungs (1).

There are two main subgroups, into which lymphoma can be divided: Hodgkin's disease, named after the doctor who was the first to describe it, and non-Hodgkin lymphoma (NHL), including lymphoma that differ in their characteristics from Hodgkin's disease (1). Characteristic for Hodgkin's disease, also called Hodgkin lymphoma, is the fact that the malignant cells, which originate from B-cells and are referred to as Hodgkin and Reed-Sternberg cells, constitute only a minority of the tumor and are accompanied by a reactive inflammatory background (5). Hodgkin's disease can nowadays be treated by well-established methods, and the cure rate is very high. In contrast, for NHL, the treatments and cure rates vary, and a lot of research is conducted to find better or new treatments (1).

NHL, which accounts for the majority (around 90%) of all lymphomas, includes a wide diversity of neoplasms of the immune system. Clinically, it usually presents with painless lymphadenopathy and possible additional systemic symptoms like fever or night sweat. Around 85-90% of NHLs originate from B-cells, the rest from T-cells or NK-cells (6).

1.1.2 Diffuse large B-cell lymphoma (DLBCL) – General overview

1.1.2.1 Incidence, pathology and clinics

The most common subtype of NHL is DLBCL (6). In Western countries, it accounts for about 31% of all NHL. The median age of affected patients lies between the 6th and 7th decade. The disease is characterized by large cells with prominent nucleoli, vesicular nuclei and basophilic cytoplasm that usually exhibit a high proliferation rate. DLBCL can arise *de novo*, but can also constitute a progression

or transformation of less aggressive B-cell neoplasms, like, e.g., follicular lymphoma (FL) (7).

To establish a diagnosis, a tissue biopsy has to be taken. Staging is a critical next step. The standard system for staging DLBCL has been suggested at the Ann Arbor Conference and the Cotswolds modification, and takes into account the number of involved sites as well as their relation to the diaphragm, the presence of so called B symptoms (fever, night sweat, body weight loss) and the existence of extranodal disease (7). Although this aggressive disease can be cured by chemo-immunotherapy in a large number of patients, 40% still succumb to their disease. One reason for this is the big heterogeneity of the malignancy (8).

1.1.2.2 The heterogeneity of DLBCL

In 2000, Alizadeh *et al.* were the first to identify the “germinal center B-like DLBCL” (GCB)-DLBCL and the “activated B-like DLBCL” (ABC)-DLBCL subtype by gene expression analysis (9). These two subtypes were later translated into routine pathology by Hans *et al.*, distinguishing the GCB-DLBCL and non-GCB-DLBCL (later in the text referred to as nGCB-DLBCL) subtype by immunohistochemistry (IHC). Importantly, the GCB-DLBCL subtype is in general characterized by a considerably better patient survival (10). In the following years, also other IHC algorithms for distinguishing the subtype were developed, for example the Choi algorithm or the Tally algorithm (11). Moreover, further gene expression profiling also identified a third subgroup of DLBCL, namely primary mediastinal B-cell lymphoma (12). It was also only recently that a different approach investigating genomic abnormalities identified four different genetic DLBCL subtypes (termed MCD, BN2, N1 and EZB) that differ in their response to immuno-chemotherapy (13). Regarding the heterogeneity of DLBCL, it is finally important to mention also two particular subgroups of DLBCL: DLBCL with an *MYC* rearrangement together with a *BCL2* and/or *BCL6* rearrangement is referred to as double-hit or triple-hit lymphoma, respectively. Additionally, DLBCL with protein overexpression of MYC and BCL-2 not related to chromosomal rearrangements is called double-expressor lymphoma. Both groups are characterized by poor patient outcome (14).

An important role in the heterogeneity of DLBCL is played by molecular pathways in the cell of origin, the B-cell, itself (15). Therefore, to understand the pathologic

mechanisms supporting DLBCL, it is important to have knowledge about B-cell function and development.

1.1.3 The B-cell

1.1.3.1 B-cell function, development and differentiation

B-cells are part of the adaptive immune system. Their major function is the production of antibodies directed against foreign antigens/pathogens (16). Despite this well-known role, there also exist further fundamental functions of B-cells: Studies with B-cell depleted mice show that B-cells are, e.g., crucial for the organogenesis of Peyer's patches (17) and the development and function of the splenic marginal zone (18). However, B-cells are not only important for normal immune system development, but also for its maintenance: for example, B-cell secreted cytokines take part in the wound healing process (19) and in naïve $CD4^+$ T-cell differentiation (20). Moreover, through antigen presentation, B-cells are also crucial for regular T-cell function by allowing for the generation of effector and memory T-cells (21).

Presumably owing to the considerable amount of B-cell functions, their development is rather complex (**Figure 1** and **Figure 2**). In general, B-cell development occurs in differentiation stages characterized by the distinct structure of the B-cell receptor (BCR). Early B-cell development takes place in the bone marrow and is completed when a functional surface antigen receptor is formed by immunoglobulin (Ig) light- and heavy-chain rearrangement (V(D)J recombination). B-cell precursors, which do not express a BCR, go into apoptosis, but cells with a functional and non-autoreactive BCR develop into mature naive B-cells and leave the bone marrow. By antigen binding to the BCR, mature naive B-cells can become activated and take part in immune responses.
Further change of the BCR takes place in structures called germinal centers (GCs) of secondary lymphoid organs such as lymph nodes (22). In these areas, antigen-activated B-cells experience clonal expansion in T-cell-dependent immune responses, and modification of Ig genes occurs by somatic hypermutation (SHM) and class switch recombination (CSR), which allows for the production of antibodies with increased antigen affinity and effector functions best suited for a particular pathogen or setting (22, 23). B-cells, which thereby acquire mutations in

the BCR increasing their antigen affinity, are positively selected. These GC B-cells finally differentiate into plasma cells or memory B-cells (22).

As mentioned above, there are three cellular programs – V(D)J recombination, SHM and CSR - to enable BCR/antibody generation. These programs work with mutations and double strand breaks and therefore cause considerable genomic alteration at Ig genes (22, 23). They are the focus of the following two chapters.

1.1.3.2 Generation of initial Ig diversity – V(D)J recombination

BCRs are membrane-bound Igs. They consist of two heavy chain and two light chain molecules. Initial diversity of the BCR is realized by a somatic recombination process, called V(D)J recombination (**Figure 1**). This recombination process brings together one segment each of the multiple variable (V), diversity (D), and joining (J) segments of the Ig heavy chain locus and fulfills the same function with the V and J segments of the Ig light chain locus. Through random insertion or deletion of nucleotides at the segment junctions, additional sequence diversity is generated within this process (24). The somatic recombination is mediated, amongst others, by the VDJ recombinase (composed of RAG1 and RAG2), an enzyme that is only produced in immature B- and T-lymphocytes. In the following primary transcript, the VDJ exon of the heavy chain locus is spliced to the first constant (C)-region exons (μ chain), giving rise to a μ mRNA. Translation results in the μ heavy chain, which is later associated with a light chain to form the IgM antigen receptor. V(D)J recombination and the associated maturation of B cells occurs primarily in the bone marrow and is associated with selection processes that favour B-cells with intact receptors and prevent self-reactive B-cells (25).

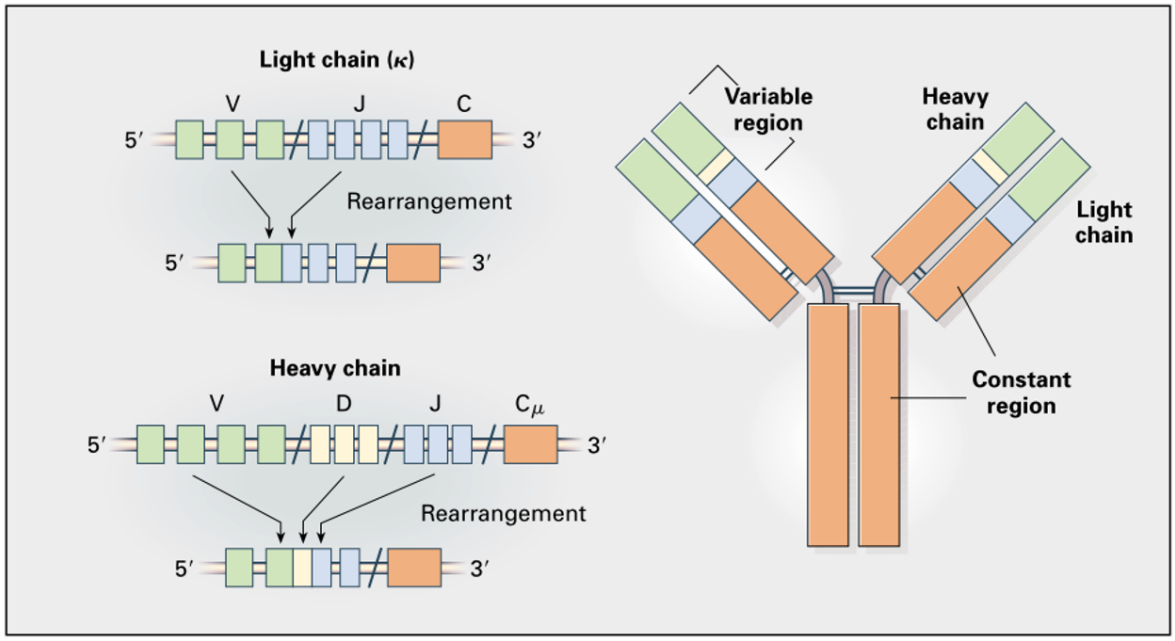

Figure 1: Schematic representation of V(D)J recombination to generate Igs. Reproduced with permission from (26), Copyright Massachusetts Medical Society.

1.1.3.3 GCs – The areas where Ig genes get remodeled

B-cells that express functional BCRs travel as naive B-cells from the bone marrow to secondary lymphoid organs. When meeting an antigen, they become activated by interaction with $CD4^+$ T-cells in the T-cell-rich area of the lymphoid organs. Subsequently, they aggregate into primary follicles to form GCs. Characteristic for GCs are Ig gene remodeling processes targeting B-cells to generate cells that are able to produce high-affinity antibodies of different isotype classes. As mentioned above, these gene remodeling processes are SHM and CSR (15).

Both processes are initiated by AID. This small protein usually deaminates cytidine residues by using preferred sequence motifs, which is then converted to double strand break and/or mutational outcomes by cellular repair mechanisms.

In brief, SHM leads to variations of the variable region of Ig light and heavy chains, which enables the selection of B-cells producing antibodies with increased antigen affinity. In contrast, CSR alters the constant region of the Ig heavy chains through a DNA double-strand-break dependent process. This leads to the generation of B-cells that produce antibodies with different Ig heavy chain effector functions that are best suited for elimination of a particular pathogen or in a particular set-up (23). At the end the outcome of the GC reaction is the generation of memory B-cells and plasma cells (15).

Based on classical histological definitions, GCs are composed of a dark zone, including highly proliferating B-cells and a light zone that contains B-cells in a mixture with follicular dendritic cells, T-cells and macrophages (compare **Figure 2**). From a functional point of view, the dark zone is the area of B-cell division and SHM, whereas the light zone is the area of B-cell selection and activation based on affinity of the BCRs (15).

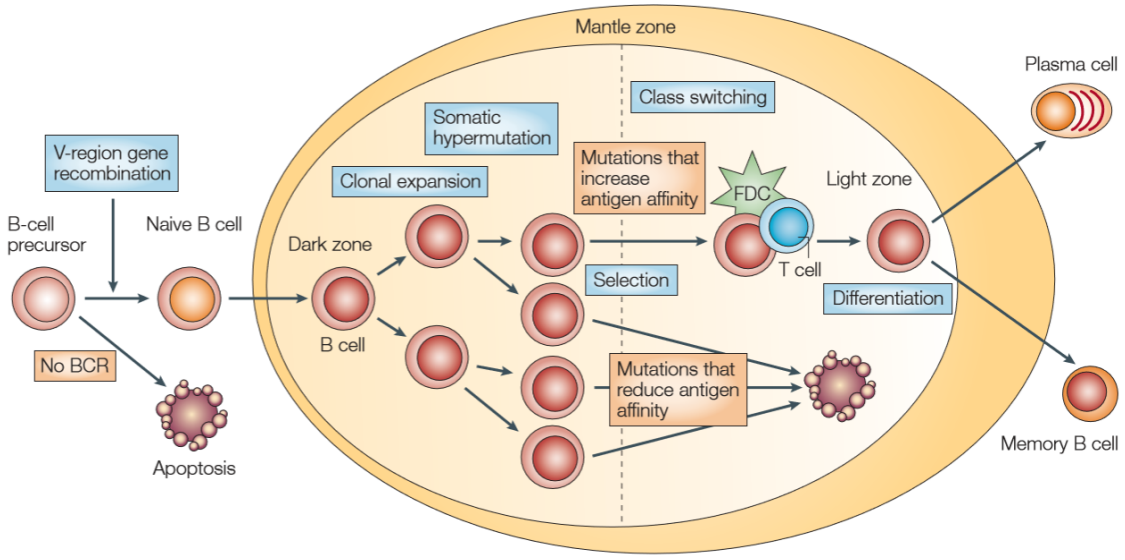

Figure 2: Schematic representation of B-cell development with GC reaction. BCR: B-cell receptor, FDC: follicular dendritic cell; Reproduced from (22) with permission of publisher Springer Nature: Reprinted by permission from Springer Nature Customer Service Centre GmbH: Springer Nature Nature Reviews Cancer (22), 2005.

1.1.4 The GC and lymphomagenesis

Many subtypes of B-cell NHL show somatically mutated Ig genes, among them DLBCL. This indicates that they originate from GC or post-GC B-cells (15, 26). DLBCL corresponds to B-cells that have been arrested by transformation events occurring at various stages of the GC transit. While the GCB-DLBCL subtype is similar to light zone B-cells, the ABC-DLBCL subtype seems to originate from GC cells that have been arrested during the early stages of post-GC plasma cell differentiation (15).

Importantly, it is often the same cellular pathways that regulate GC formation and maintenance that are also involved in the malignant transformation process, which

leads to lymphomagenesis (15). Therefore, knowledge about them is important to understand DLBCL pathogenesis.

Various transcription factors and modulators play a role in the regulation of the fundamental GC processes of GC initiation, expansion and exit. **Figure 3** provides an overview of these transcriptional networks that drive the GC reaction. Importantly, most of the factors involved are not expressed throughout the whole GC life of B-cells, but rather show a GC phase-specific pattern, which is linked to their function. Often the transcription factors are moreover also involved in mutual transcriptional modulation. An example of this is *MYC*, which is induced early during GC initiation, is then transcriptionally repressed in dark zone B-cells by the GC master regulator BCL-6, followed by transient re-expression in a subgroup of light zone B-cells (15).

The aforementioned two factors and their interaction are, however, only examples and far more play a role during the GC reaction (see **Figure 3**). Importantly, these effectors can be targeted by genetic alterations which change their orderly function (15). Some of the factors and their alterations are, therefore, discussed in the following chapter, which focuses on their role in DLBCL.

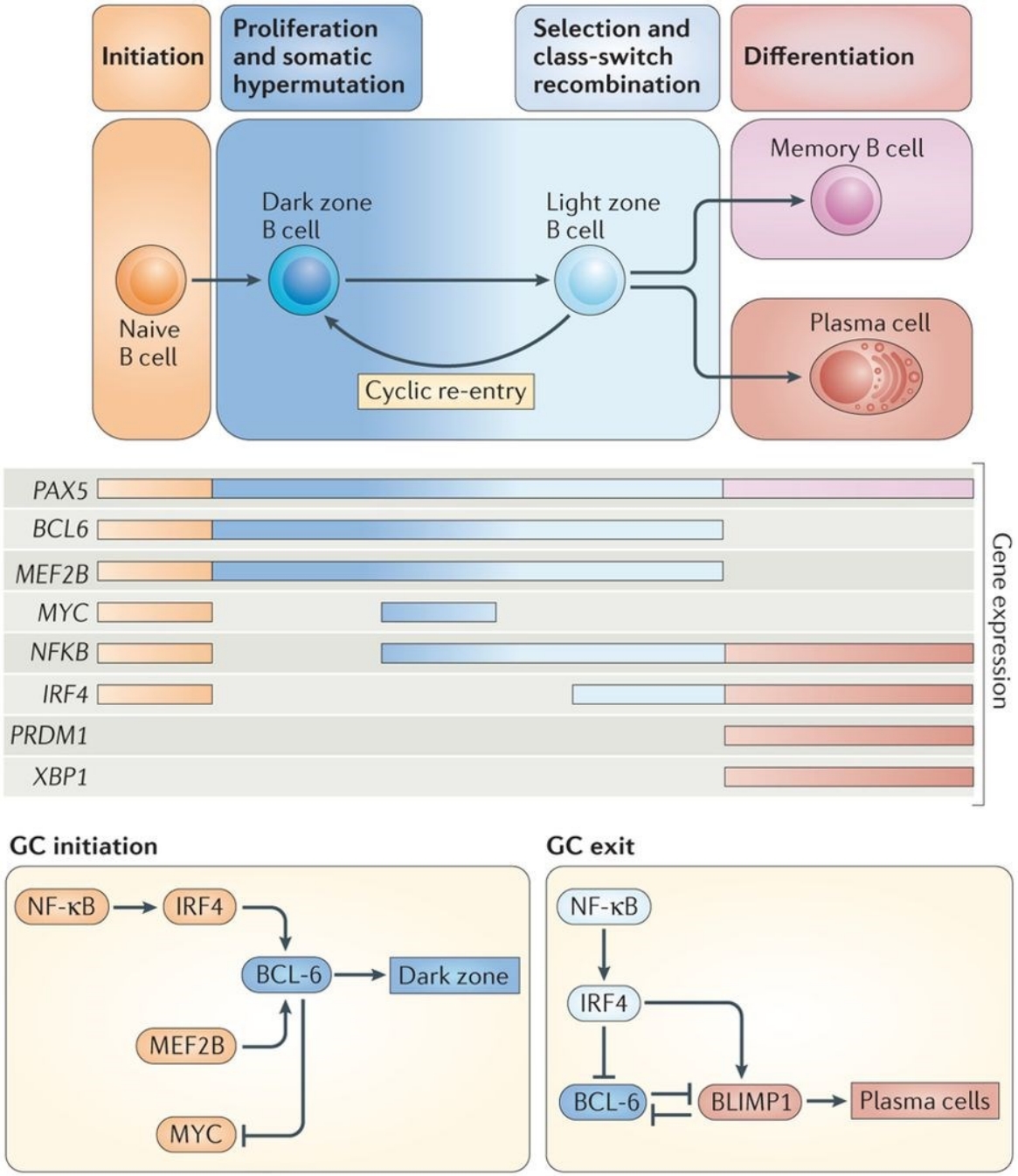

Figure 3: Transcriptional networks that drive the GC reaction. Reproduced from (15) with permission of publisher Springer Nature: Reprinted by permission from Springer Nature Customer Service Centre GmbH: Springer Nature Nature Reviews Immunology (15), 2015.

1.1.5 The biology of DLBCL

1.1.5.1 Genetic lesions in DLBCL

DLBCL has an average somatic frequency of 4-5 mutations/Megabase. This is a higher rate than that in acute leukemia, but a lower one than that in e.g. melanoma. Across DLBCL subtypes, most genetic alterations are not randomly distributed. Therefore, although the subtypes share some of them, they are also characterized by specific genetic alterations (27).

1.1.5.1.1 Genetic aberrations shared by the GCB-DLBCL and ABC-DLBCL subtype

In general, DLBCL often displays alterations in chromatin modifiers, e.g. frequent structural alterations that inactivate the two highly related histone and non-histone acetyltransferases CREBBP and EP300. Even about 39% of DLBCL cases harbor somatic mutations and/or genomic deletions inactivating or removing the acetyltransferase coding domain of these two genes. Mutant CREBBP and EP300 proteins lead to constitutive activation of BCL-6 and to decreased p53 tumor suppressor activity by being deficient in acetylating BCL-6 and p53. This therefore indicates a major pathogenetic mechanism of DLBCL (28).

However, BCL-6 itself, a protooncogene predominantly expressed in GC B cells and working as a transcriptional repressor, also plays a very important role in DLBCL pathogenesis (29). Under normal conditions, BCL-6 is required for the GC reaction in mature B-cells. It enables an environment that is tolerant of the DNA breaks accompanying the remodeling processes of Ig genes and prevents GC B cells from premature activation and differentiation (30). The two major types of molecular alterations targeting the *BCL6* gene are SHM and translocations. Mutations and translocations affect thereby both molecular DLBCL subtypes (29). Dysregulated BCL-6 plays a crucial role in lymphomagenesis by suppressing DNA damage responses, enforcing the proliferative phenotype of GC B-cells and hindering terminal differentiation. Overall, genetic alterations affecting the *BCL6* locus and triggering its dysregulated expression are seen in ~30% of DLBCL cases (15).

Another important mechanism in DLBCL supporting both subtypes is its immune escape. DLBCL cells often do not express surface molecules necessary for recognition by immune-effector cells. In 29% of cases, the *B2M* gene is inactivated by mutations or deletions, in 21% of the cases, genetic lesions affect the *CD58* gene. These genes are necessary for tumor cell recognition by T-cells and NK-cells, with B2M being a subunit of MHC class I and CD58 a highly glycosylated cell adhesion molecule interacting with T-cells and NK-cells, respectively (31). Moreover, other functionally-related genes and their products can also be affected (15).

FOXO1 is a transcription factor specifically expressed in the GC dark zone and essential for dark zone formation (32). Interestingly, in 9% of DLBCL cases, mutations of the respective gene (*FOXO1*) were found, and *FOXO1* mutation was linked to decreased overall survival (33). A systematic functional analysis of the consequences of *FOXO1* mutations in the context of B-cells is at the moment lacking, although it has been suggested that the mutations prevent inactivation of FOXO1 by PI3K signaling (34).

1.1.5.1.2 Genetic aberrations predominantly affecting the GCB-DLBCL subtype

BCL-2 is an important antiapoptotic molecule that is expressed in most tissues, but not in the GC. However, approximately 30% of GCB-DLBCL harbor the t(14;18) translocation, which brings the coding exons of *BCL2* under the control of the *IG* locus. This leads to the ectopic expression of *BCL2*. The deregulation of BCL-2 has been linked to worse outcome, particularly when coupled with deregulation of MYC, a transcription factor involved in multiple biological functions, such as apoptosis or proliferation. *MYC* transcription is suppressed in most GC B-cells. Often as a result of chromosomal translocations joining its coding domain to Ig chain loci, *MYC* shows ectopic and constitutive expression in 10% to 14% of GCB-DLBCLs. Again, these translocations have been linked to worse patient prognosis in DLBCL. Chromosomal translocations of *BCL2* and *MYC* (or, less often, *BCL6*) occurring at the same time are found in 5% to 10% of DLBCL, and are referred to as double-hit lymphoma (see also the general overview of DLBCL) (34).

In approximately 22% of GCB-DLBCLs the *EZH2* gene is mutated (35). EZH2 is a histone methyltransferase that is highly expressed in GC B-cells. It works by repressing proliferation checkpoint genes and transiently suppresses GC B-cell differentiation. These effects are reinforced by somatic mutations as the silencing of the targets is enhanced in this set-up. In line with this, conditional expression of mutant EZH2 leads to GC hyperplasia in mice and induces accelerated lymphomagenesis in cooperation with BCL-2 (36).

GNA13, the gene encoding Gα13, is mutated in 15-33% of GCB-DLBCLs. Gα13 is central to a pathway that suppresses growth and also blocks dissemination of GC B-cells. Normally, GC B-cells are tightly regulated in growth and restricted to the GC. This characteristic is lost in GCB-DLBCL, and disruption of Gα13 signaling by mutations in *GNA13* and other related genes engaged in this signal pathway seems to contribute to this loss (37).

1.1.5.1.3 Genetic aberrations predominantly affecting the ABC-DLBCL subtype

The ABC-DLBCL subtype of DLBCL is dependent on constitutive activity of NF-κB (38) and is particularly characterized by alterations converging onto the NF-κB-pathway. For example, somatic mutations affecting signaling modules of CD79A and B, which mediate BCR signaling to downstream pathways like the NF-κB-pathway, are frequently seen in ABC-DLBCL. In 18% of ABC-DLBCLs, a critical residue of CD79B is mutated. In contrast, this event is very rarely seen in GCB-DLBCL. It has been shown that these mutations increase BCR expression on the surface and attenuate inhibition of BCR signaling (39). Furthermore, approximately 10% of ABC-DLBCL harbor missense mutations in the gene coding for CARD11, another signal transducer between antigen stimulation and the NF-κB-pathway. This seems to lead to constitutive NF-κB-activation and enhanced activity of NF-κB upon antigen receptor stimulation (40). Another genetic lesion affecting the NF-κB-pathway involves the *A20* gene, a negative regulator of NF-κB. Its product is involved in termination of NF-κB responses. In approximately 30% of patients, biallelic inactivation of this gene by mutations and/or deletions occurs (41). The *MYD88* gene is also often mutated. 29% of ABC-DLBCL tumors show a particular

amino acid substitution (L265P), a gain-of-function driver mutation leading, amongst others, to NF-κB-signaling (42).

Another important mechanism in ABC-DLBCL, other than those affecting the NF-κB pathway, involves Blimp-1. By blocking the expression of genes involved in cell proliferation and BCR signaling, Blimp-1 is crucial for the terminal differentiation of GC B-cells into plasma cells. It has been shown that the respective gene *BLIMP1* is inactivated by structural alterations in approximately 25% of ABC-DLBCLs (43). Using a mouse model, abrogation of terminal B cell differentiation through *BLIMP1* disruption and constitutive NF-κB-activity have been shown to cooperate in lymphomagenesis (44).

Furthermore, gains of chromosome 3 are characteristic for ABC-DLCBCL. 15% of ABC-DLBCLs have trisomy 3, and 26% gains of the whole 3q arm (45). For example, *BCL6* is located on chromosome 3 and is known to be deregulated in this DLBCL-subtype. However, the lesions are generally very large, what indicates that more than one gene might be implicated in lymphomagenesis (27).

Table 1 summarizes the frequent genetic alterations in DLBCL described above.

Table 1: Frequent genetic alterations in DLBCL separated by DLBCL subtype (15, 34, 45).

Affecting the GCB-DLBCL and ABC-DLBCL subtype	**Predominantly affecting the GCB-DLBCL subtype**	**Predominantly affecting the ABC-DLBCL subtype**
Alterations in chromatin modifiers (*CREBBP* and *EP300*)	Alterations in *BCL2* and *MYC*	Alterations affecting the NF-κB-pathway (e.g. *MYD88*)
Alterations in *BCL6*	Alterations in *EZH2*	Alterations in *BLIMP1*
Immune escape (*B2M* and *CD58* alterations)	Alterations in *GNA13* and related genes	Gains of chromosome 3
Alterations in *FOXO1*		

Recently, a novel study revealed four genetic subtypes of DLBCL based on genetic aberrations (see also the general overview of DLBCL). The subtypes are characterized, amongst others, by mutations of *CD79B*, *MYD88* or *EZH2*, genetic aberrations also mentioned above. Furthermore, also mutations in *NOTCH1* and

NOTCH2 were shown to be characteristic for specific subtypes. Importantly, the genetic subtypes revealed different gene-expression signatures and, most importantly, different patient outcome (13). This study thereby underlines once more the importance of genetic aberrations in DLBCL pathogenesis and the ongoing research in this field.

1.1.5.2 The role of the tumor microenvironment in DLBCL

Today it is known that elements of the tumor microenvironment enable cancer pathogenesis and progression and are not only bystanders or part of the host antitumor response (46). For example, gene expression profiling has shown that signatures derived from the tumor microenvironment can also predict DLBCL patient outcome. The favorable stromal-1 signature was thereby related to histiocytic infiltration and extracellular-matrix deposition, and the unfavorable stromal-2 signature was related to tumor blood-vessel density (47). However, compared to other lymphomas, such as FL, the tumor microenvironment seems to play a less important or an at least understudied role in DLBCL. Presumably, this is also due to its mutational landscape, enabling relative independence from the microenvironment by mutations that give, e.g., rise to chronic NF-κB-activation (46).

1.1.6 Established and currently tested new therapeutic options in DLBCL

Treatment of DLBCL patients has been mainly based on CHOP (stands for cyclophosphamide, doxorubicin, vincristine, and prednisone) chemotherapy. However, outcomes improved considerably when the monoclonal anti-CD20 antibody rituximab was added to this chemotherapy backbone. This led to the establishment of R-CHOP as the standard of care. In the salvage setting, in which autologous stem cell transplantation is important, only a relatively small number of patients are cured. Research on the biological heterogeneity of DLBCL has revealed new therapeutic targets and has led to the development of novel agents, which could provide an alternative for R-CHOP or help in the refractory/relapsed setting (48).

As such, ibrutinib is currently tested in DLBCL. This agent is an inhibitor of BTK, a component of the BCR signaling pathway. The patients' response thereby depends on the DLBCL-subtype, with a higher response rate in ABC-DLBCL patients (49). This is in accordance with the importance of BCR signaling in ABC-DLBCL also mentioned above (39). Furthermore, also BCL-2 family members represent appealing targets in lymphoma therapy. In this regard, Venetoclax, a selective inhibitor of BCL-2, is tested as a possible new agent in DLBCL treatment. Lenalidomide is the lead compound in the class of immunomodulatory drugs. These agents, amongst others, increase the actions of immune-effector cells. Their true potential might thereby lie in the incorporation into new combination regimens which are also currently being tested for Lenalidomide in DLBCL patients (49).

1.1.7 Prognostic factors for DLBCL currently used in the clinics

The gold standard as clinical prognostic tool in DLBCL, in the past and still at present, is the International Prognostic Index (IPI) (50, 51). This prognostic index, first published in 1993, is based on age, performance status, tumor stage, serum lactate dehydrogenase concentration and number of extranodal disease sites, and separates patients into four risk groups (51). Moreover, there are also further prognostic factors today that are based, for example, on the genetic profile of DLBCL and thus take the DLBCL biology into account. As such, the currently recommended standard prognostic factors are as follows:

- the IPI
- IHC for cell of origin
- positron emission tomography (PET)/computed tomography (CT) scan (with a positive PET/CT scan at end of treatment being associated with inferior survival) and
- testing for *MYC* and *BCL2* rearrangements by Fluorescent *in situ* hybridization (50).

Of note, although clinical factors are surrogates for biological features, no biological marker has been able to render the IPI redundant so far (48).

1.2 Eukaryotic initiation factors (eIFs)

1.2.1 Eukaryotic translation initiation and eIFs

The process of gene expression is regulated at various levels. One of these is the translation of mRNAs into proteins (52). A central role in this step is played by ribosomes, which translate transcribed mRNAs into polypeptide chains (53). The translation process can be divided into four stages: initiation, elongation, termination and ribosome recycling. Importantly, its regulation occurs primarily at the first stage (52). The function of translation initiation is to build an elongation-competent 80S ribosome out of the large 60S and small 40S ribosomal subunits, which has the initiator methionyl-tRNA (Met-$tRNA_i$) located over the start codon of the mRNA (54). Realization of this function is supported by at least 12 eIFs (52, 54).

The start of translation initiation is marked by the formation of a ternary complex composed of eIF2, GTP and Met-$tRNA_i$. The ternary complex then forms a pre-initiation complex (PIC) with eIFs 1, 1A, 3 and 5 and the 40S ribosomal subunit. This complex is subsequently loaded onto the 5´ end of the mRNA, which is marked by a 7-methylguanosine cap, by a lot of different factors, including eIF3, eIF4E, eIF4A and eIF4G. In brief, eIF4E recognizes the 5´-cap structure and recruits, together with RNA binding sites in eIF4G, the RNA helicase eIF4A to the 5´ untranslated region (5´ UTR) of the mRNA. By unwinding structures in the 5´ UTR, eIF4A can now pave the way for the incoming PIC. Importantly, through interaction, amongst others, with eIF4E, eIF4G can bring both ends of the mRNA (5´ and 3´) together. The resulting “closed-loop messenger ribonucleoprotein (mRNP)” is believed to be activated for interaction with the PIC. Subsequently, after loading onto the mRNA, the PIC is thought to scan the 5´ UTR of the mRNA for the start codon, and upon recognition of the start codon, the PIC changes to a “closed confirmation” triggered by the action of eIF1, eIF2 and eIF5 (amongst others through change of eIF2 to its GDP-bound state). This “closed confirmation” of the PIC stops the scanning process. The 60S subunit joins and the 80S initiation complex is assembled, mediated by eIF5B and eIF1A, and after release of eIF5B and eIF1A, the ribosome can enter the subsequent elongation phase (54). Of note, besides cap-dependent translation described above there are also

cap-independent translation mechanisms known, but these are not the focus of this dissertation (55).

Figure 4 depicts a schematic representation of the above described translation initiation pathway. Additional information about the function of specific eIFs is moreover provided in the following chapters.

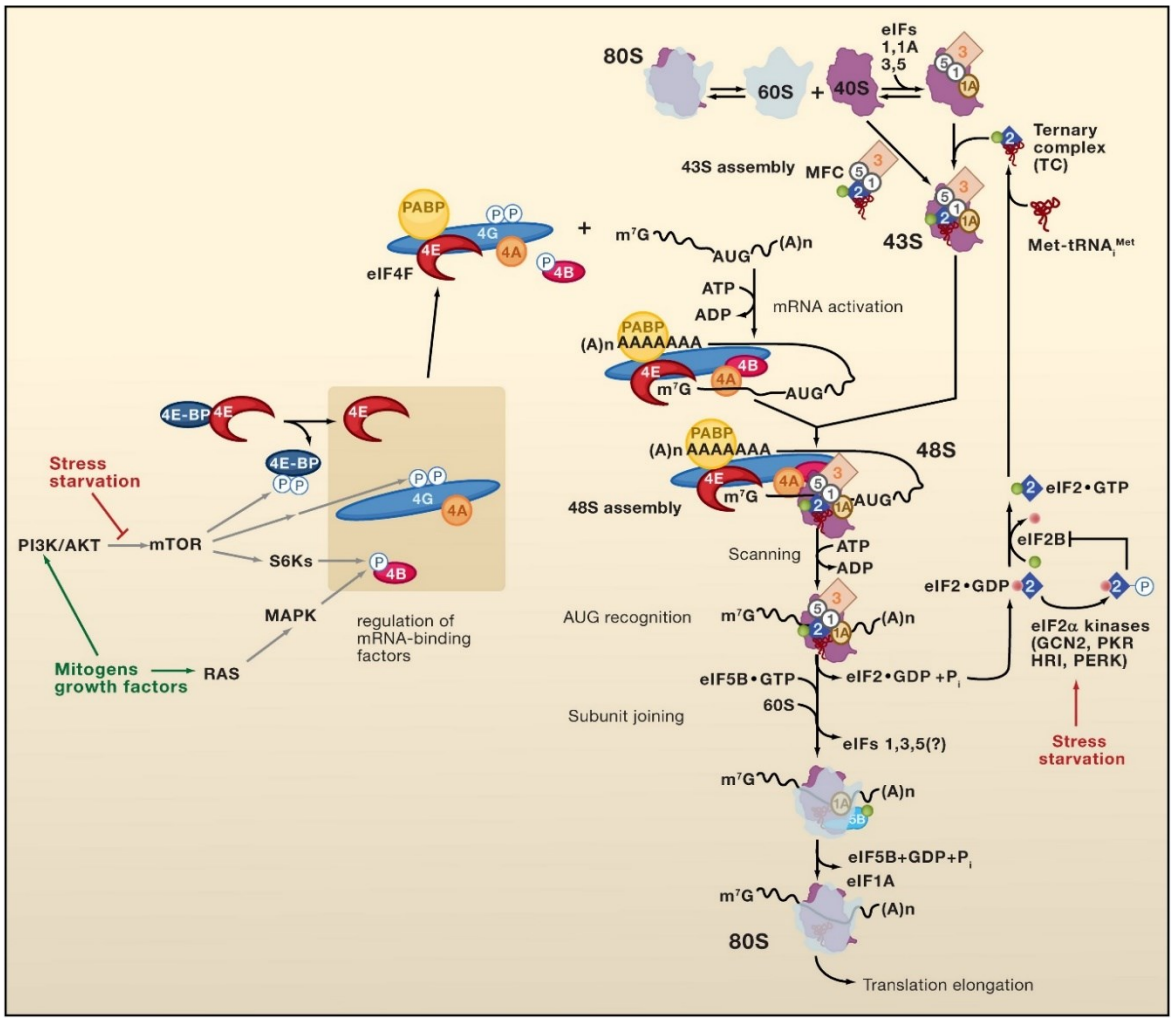

Figure 4: Schematic representation of translation initiation in eukaryotes. Reprinted from (52), Copyright (2009) (and (56), Copyright (2007), respectively), with permission from Elsevier.

1.2.2 eIFs and cancer

Importantly, in the pathological setting, dysregulation of mRNA translation is observed, and eIFs have been shown to be critically involved in various oncogenic processes, with aberrant eIF activity being linked to tumor initiation and also progression (57, 58). Therefore, the following chapters are dedicated to the role of

different eIFs in cancer, highlighting their very important contribution to various cancer entities.

1.2.2.1 eIF4-factors

The eIF4-factors eIF4E, eIF4A and eIF4G are generally summarized to the eIF4F-complex. The eIF4F-complex and a few additional factors recognize the mRNA (eIF4E), unwind it (mainly eIF4A) and recruit it to the PIC (presumably through interaction with eIF3) (54).

Nearly 30 years ago, Lazaris-Karatzas *et al.* reported that overexpression of the mRNA cap binding factor eIF4E led to the tumorigenic transformation of cell lines (59). The oncogenic nature of eIF4E was subsequently confirmed by multiple studies (reviewed in (57)). Accordingly, eIF4E overexpression has been reported in various human tumor entities, e.g. in breast, prostate, lung, bladder or cervix cancer, and eIF4E function has also been associated with metastasis (60). Interestingly, mRNAs with long and structured 5'UTRs seem to be particularly sensitive to changes in eIF4E levels. The majority of these mRNAs encode tumor-promoting proteins, including, amongst others, MYC. Therefore, eIF4E appears to drive carcinogenesis by selectively enhancing the synthesis of tumor-promoting proteins. Nevertheless, the exact set of eIF4E-sensitive mRNAs still is a matter of debate and ongoing research. Moreover, besides the above described oncogenic role of eIF4E, modification of eIF4E by phosphorylation has also been linked to tumorigenesis and tumor progression. It seems that phospho-eIF4E thereby also selectively increases the translation of a specific set of mRNAs (encoding, e.g., prosurvival proteins like MCL-1), which, however, only partially overlaps with that linked to overexpression of eIF4E (57).

An important binding partner of eIF4E is 4E-BP1. This protein binds to eIF4E and inhibits its complex assembly. Importantly, 4E-BP1 is regulated by the mTOR signaling pathway. Upon activated mTOR signaling pathway, 4E-BP1 becomes phosphorylated, releases eIF4E and thereby enables translation initiation, depicting a mode how cellular signaling pathways affect eIFs (61). Phosphorylated 4E-BP1 has been associated with adverse cancer phenotypes, e.g., in breast cancer, where it has been linked to the presence of lymph node metastasis and locoregional recurrences (62). Accordingly, accumulating evidence suggests

phosphorylated 4E-BP1 to be a marker for worse patient outcome, see e.g. (63). Interestingly, total 4E-BP1 has also been linked to poor cancer patient survival and has been revealed to be overexpressed in cancer compared with non-neoplastic controls, as shown in hepatocellular carcinoma for example (61).

eIF4G is a big scaffold protein that holds several important interactions for mRNA preparation and recruitment to the PIC. There are two isoforms in mammals, eIF4GI and eIF4GII, and furthermore a paralog, DAP5, that is suggested to participate in cap-independent translation (57). Similarly to eIF4E, overexpression of eIF4GI has also been shown to lead to malignant transformation of NIH3T3 cells (64). Moreover, eIF4GI is also overexpressed in human cancer, such as inflammatory breast cancer (57, 65). Thereby, eIF4GI dysregulation seems to selectively modulate cap-dependent and cap-independent translation of mRNAs (57). At present, about the remaining eIF4G isoform and paralog not that much is known.

eIF4A is an ATP-dependent RNA helicase that unwinds the mRNA. It represents the enzymatic core of the eIF4F-complex (54, 57). There are again two paralogs of eIF4A: eIF4AI and eIF4AII (57). Studies have elucidated the role of eIF4AI and eIF4AII in several cancer entities, including melanoma, breast and lung cancer (66-68).

Finally, eIF4B and eIF4H are two accessory proteins to the eIF4F-complex. (57) They stimulate the unwinding of RNA by eIF4A (54). Importantly, these two eIFs have also been linked to oncogenic processes, see e.g. (69, 70).

1.2.2.2 eIF1 and eIF1A

Both factors, eIF1 and eIF1A, are required for initiation complex assembly and mRNA screening for the start codon (58).

Of note, gene expression of *EIF1* has been shown to be upregulated by genotoxic and ER-stress (71). Compared to non-tumor liver, eIF1 is downregulated in hepatocellular carcinoma. Accordingly, eIF1 introduction into HepG2 cells leads to an inhibition of cell growth and partial inhibition of tumor formation in nude mice (72). In contrast, however, Golob-Schwarzl *et al.* recently reported that compared to non-neoplastic controls, eIF1 expression was higher in colon and rectum

carcinoma (73), indicating a potential cell context-specific function and a not yet fully elucidated role of eIF1 in carcinogenesis.

Recently, a function of eIF1A outside of translation initiation was reported: eIF1A was shown to interact with Ago2 and to promote its activities in miRNA biogenesis and miRNA-guided RNA interference. It was thereby proposed that eIF1A is a component of the Ago2-centred RNA-induced silencing complexes (74). Regarding the neoplastic setting, eIF1A has been frequently shown to be genetically mutated in different cancer entities, including, e.g., uveal melanoma and thyroid carcinoma (75, 76). Importantly, subsequent molecular studies suggested that these mutations seen in uveal melanoma alter gene expression by enhancing the selection against poor initiation sites during translation initiation (77). Besides genetic mutations, however, not that much is currently known about the role of eIF1A in cancer.

1.2.2.3 eIF2 and its regulatory cycle

The loading of the Met-tRNA$_i$ onto the small ribosomal subunit requires the action of initiation factor eIF2. eIF2 is a heterotrimer consisting of the α-, β- and γ-subunit (54). Importantly, it is a GTP-binding protein, and only when eIF2 is in its active GTP-bound state, it binds to the Met-tRNA$_i$ before it subsequently forms the PIC together with other initiation factors and the small ribosomal subunit (see **Figure 5**). The PIC then screens the mRNA for the start codon. Upon start codon recognition, eIF2-bound GTP is hydrolyzed. This is triggered by the GAP (stands for GTPase accelerating protein) activity of another initiation factor, namely eIF5. Subsequently, eIF2-GDP in complex with eIF5 is released from the initiation complex, and eIF5 now functions as a GDI (stands for GDP dissociation inhibitor), thereby blocking premature release of GDP. Consequently, to enable further rounds of translation initiation, eIF2 has to be reactivated. At this stage, eIF2B, a GEF (stands for guanine nucleotide exchange factor), comes into play (78). This important factor consists of five subunits (α-ε), which assemble into a complex consisting of two copies of each subunit. The ε-subunit holds the catalytic center of the enzyme and is associated with the γ-subunit, while the α-, β- and δ-subunits have regulatory functions (79). eIF2B now exchanges the eIF2-bound GDP to

GTP, and eIF2 is reactivated so that it can rebind Met-tRNA$_i$. Thus, the GAP, GDI and GEF activities executed by eIF5 and eIF2B control the activity of eIF2 (78).

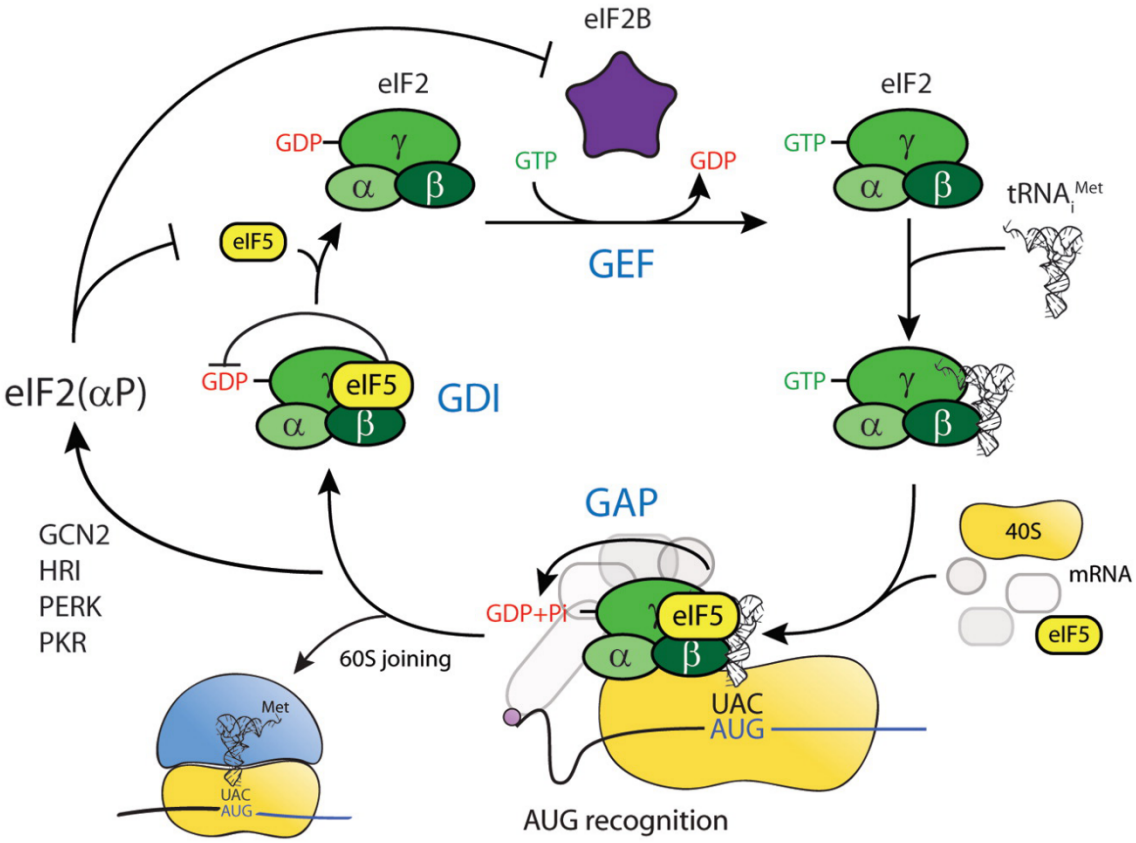

Figure 5: Schematic representation of the regulatory cycle controlling eIF2-function. Reproduced from (78). Shown is one of three panels of the original figure. [https://creativecommons.org/licenses/by-nc/3.0/]

Importantly, the α-subunit of eIF2 can be phosphorylated, what plays a prominent role under stress conditions. eIF2α phosphorylation thereby inhibits the GEF activity of eIF2B, what, in turn, impedes eIF2-GDP recycling (compare also **Figure 5**). Although this inhibits global protein synthesis, it stimulates the translation of specific stress response mRNAs. Phosphorylation of eIF2α is an important step in the integrated stress response, which is suggested to be a crucial cytoprotective mechanism activated by various stressors like ER-stress or double-stranded RNAs. However, it is not completely clear which role eIF2α phosphorylation plays in the neoplastic setting, although there are multiple studies investigating this question. Targeting this pathway in cancer seems to be particularly complicated by the fact that phospho-eIF2α can stimulate cell survival but also apoptosis in dependence on the type of stress, its severity and its duration (57).

Compared to the number of studies investigating eIF2α phosphorylation, only little is known about the expression profile of eIF2α in different cancer entities. Nevertheless, what is known primarily suggests an increased expression of eIF2α in the neoplastic setting, as reported for example in melanoma and bronchioloalveolar carcinoma (80, 81). Only recently, eIF2β was reported to be upregulated in lung cancer and was suggested as a novel therapeutic target (82), what clearly indicates moreover the need for further studies to better characterize the role of eIF2β and eIF2γ in different cancer entities as well.

As indicated above, eIF5 and eIF2B are crucial for controlling eIF2 activity. Thereby, eIF5 is important to trigger eIF2-GTP hydrolysis upon start codon recognition and to stabilize the resulting eIF2-GDP, which is later recycled by eIF2B yielding again active eIF2-GTP (78). Only very few studies have analyzed eIF5 in cancer (e.g., (73)). More is known about the role of eIF2B in cancer and other diseases. eIF2B is intrinsically tied to an inherited disorder called leukoencephalopathy with vanishing white matter. This progressive disorder is caused by genetic mutations in any of the five subunits of eIF2B (gene names: *EIF2B1* to *EIF2B5*, encoding eIF2Bα to eIF2Bε). Being pathologically linked, amongst others, to an increasing rarefaction of white matter and cystic degeneration, it is clinically primarily characterized by cerebellar ataxia. Importantly, in this disease, minor stress conditions like fever trigger major neurologic deterioration. Decreased eIF2B activity has thereby been linked to stress hyperreactivity (83). As mentioned above, eIF2Bε plays a particularly important role within the eIF2B-complex, since it is this subunit that is believed to confer the catalytic activity (79). Overexpression of eIF2Bε has been shown in various cancer entities, including ovarian, stomach and lung cancer (84, 85). Reduction of eIF2Bε expression in cells overexpressing eIF2Bε suppresses their transformed phenotype, as reflected by diminished cell growth rate and tumor progression in nude mice (86). Furthermore, its gene, *EIF2B5*, has been linked to patient prognosis in ovarian cancer, where rare alleles of it were associated with better patient outcome (87). In colorectal cancer, *EIF2B5* has been additionally shown to be a hub for stage-IV progression (88). Importantly, intron retention in *EIF2B5* has moreover recently been identified as a mechanism of translation

inhibition suggested to help cancer cells to adapt to hypoxic conditions (89). Because of its gene name, eIF2Bε will be in the following referred to as eIF2B5.

1.2.2.4 eIF3-complex

With approximately 700 kDa, eIF3 is the largest initiation factor. It is composed of 13 described subunits, ranging from eIF3a to eIF3m (see **Figure 6**). Within translation initiation, eIF3 fulfils a lot of different tasks, including the stabilization of ternary complex binding to the small ribosomal subunit and mRNA recruitment to it (58).

The role of various eIF3-subunits in cancer has been analyzed in multiple studies, demonstrating, e.g., cancer-associated altered expression, gene amplification and also prognostic significance, as exemplified in (90-93). Of note, not only overexpression in cancer but also downregulation of eIF3-subunits was detected, what applies, for example, to the eIF3f-subunit in pancreatic cancer, where loss of the *EIF3F* gene was reported (94). Moreover, interacting partners of eIF3-subunits have been identified. As such, eIF3c has been shown to interact with the tumor suppressor schwannomin, which is frequently lost by gene mutation events in benign human brain tumors (95). When looking at eIF3-subunits in different cancer entities, however, the differential expression does not follow a specific pattern where the different parts of the eIF3-complex could be grouped together. It might be possible that the tumor suppressive or oncogenic functions of eIF3-subunits are also determined by their actions outside the eIF3-complex (58).

Recently, one eIF3-subunit, eIF3d, attracted particular attention. It was shown that eIF3d has cap-binding activity, demonstrating a novel cap-dependent translation initiation mechanism independent of eIF4E. Cap-binding by eIF3d is thereby necessary to allow for the assembly of translation initiation complexes on eIF3-specialized mRNAs, including, e.g., cell proliferation regulator mRNAs like the one encoding c-Jun (96, 97). Importantly, similar to many other eIF3-subunits (see above), eIF3d and its altered expression have also been linked to cancer, as reported, e.g., in (98-100).

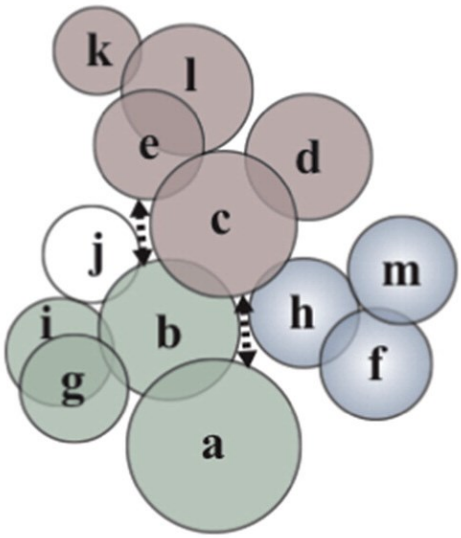

Figure 6: Structural model of mammalian eIF3 based on interactions of human eIF3-subunits. Reprinted from (101), Copyright (2015), with permission from Elsevier. Shown is one of four panels of the original figure. The reprinted figure was originally modified from (102) (Copyright (2008) National Academy of Sciences, U.S.A.) and (103) [https://creativecommons.org/licenses/by/3.0/].

1.2.3 eIFs and B-cell lymphoma with special emphasis on DLBCL

Already in 1999, Wang *et al.* investigated the expression profile of eIF2α and eIF4E by using IHC on different lymphoma entities, ranging from indolent to highly aggressive lymphomas. They detected a correlation between eIF2α and eIF4E expression and B-cell lymphoma aggressiveness, linking weak expression of these two eIFs to less aggressive lymphomas, and strong expression in contrast to more aggressive lymphomas (104). To date, several studies on the role of eIFs in lymphomagenesis have been performed, focusing particularly on eIF4-factors. Mice with eIF4E-expression under the control of the ubiquitous β-actin promotor show increased tumorigenesis, with a considerable fraction of developed tumors being B-cell lymphomas (16%). However, due to the fact that tumorigenesis occurs relatively late in these mice, Ruggero *et al.* suggested that eIF4E might cooperate with further oncogenic events in the process of tumorigenesis. Indeed, intercrossing the mice with MYC overexpressing Eμ-*Myc* mice revealed a markedly accelerated lymphoma onset in the double-transgenic animals. Further in-depth analysis showed that the cooperation of MYC and eIF4E in lymphomagenesis is based on the ability of MYC to override senescence induced by eIF4E and the complementary ability of eIF4E to suppress apoptosis triggered by MYC (105). Another oncogenic mechanism in lymphomas has been presented

by the study of Hart *et al*. They reported that human B-cell lymphoma samples characterized by MYC overexpression showed increased activation of the unfolded protein response (UPR) pathway (a cellular stress program), reflected, amongst others, by increased eIF2α-phosphorylation in comparison with B-cells from healthy donors. It seems as if activation of the UPR-pathway by MYC leads to increased cell survival by inducing cytoprotective autophagy, and protecting against apoptosis triggered by MYC induced accumulation of misfolded proteins (106). Reviewing the literature, in general, mouse lymphoma models are commonly used for analyzing the role of eIFs in tumorigenesis, in particular in the context of MYC deregulation (most often regarding eIF4-factors, as mentioned above) (107-111).

Using pull down assays in mantle cell lymphoma cell lines, Demosthenous *et al.* demonstrated that the cap bound fraction in lymphoma cells, compared to normal B-cells, was enriched with eIF4E, eIF4A and eIF4G, revealing a translationally activated state of lymphoma cells. Furthermore, analysis of a DLBCL TMA revealed eIF4E expression in 77% of patient samples, no subtype-specific expression pattern, association of eIF4E expression with higher Ann Arbor Stages and a trend between eIF4E expression and inferior event free survival (112). Moreover, in line with eIF4E's role in lymphomagenesis (105), also its overexpression in primary DLBCL and cell lines in comparison with centroblasts was reported (113). Of note, besides its levels, the phosphorylation status of eIF4E also seems to be crucial for its action in lymphomagenesis, and phospho-eIF4E has been shown to correlate with the expression of the anti-apoptotic protein MCL-1 in DLBCL (108). Another mechanistic study by Landon *et al.* investigated the role of two members of the eIF4E-family, the often investigated eIF4E1 (only referred to as eIF4E in most cases) and the more uncommon eIF4E3, directly in DLBCL. They found out that MNKs can modify oncogenic translation by regulating the activity and levels of eIF4E1 and eIF4E3 (114). In addition to eIF4E, also its repressor, 4E-BP1, has been analyzed in DLBCL. In a pure descriptive study, Kodali *et al.* analyzed various B-cell lymphomas by IHC and showed that 4E-BP1 expression was higher in most B-cell lymphoma samples tested (among them DLBCL) when compared to GCs of reactive lymphoid tissues (115). Ninan *et al.* reported in a further IHC-based study that high levels of 4E-BP1

phosphorylation were associated with worse patient outcome in low-risk DLBCL patients (116). Possibly in line with this observation, a particular role of 4E-BP1 phosphorylation in the context of MYC-driven lymphomagenesis has been described and was also proven in DLBCL with an association between high MYC expression and increased 4E-BP1 phosphorylation (117). Furthermore, other eIF4-factors have also been investigated in DLBCL and have been linked to its pathogenesis. It has been shown that eIF4GII is a target of miR-520c-3p. Interestingly, miR-520c-3p is lower expressed in DLBCL with reciprocally higher eIF4GII protein expression in comparison with normal B-cells (118). Moreover, eIF4B has been shown to be upregulated in DLBCL, presumably through mTOR signaling. Importantly, this seems to drive translation of specific mRNAs with structured 5' UTRs that, amongst others, are involved in tumorigenesis. Of note, in this study conducted by Horvilleur *et al.*, eIF4B was also linked to poor prognosis in DLBCL (119). Only recently, Kapadia *et al.* furthermore revealed that FASN through S6Kinase activity induces a complex between eIF4B and the de-ubiquitinating enzyme USP11, which promotes oncogenic translation in DLBCL, linking lipid metabolism and protein translation in this neoplastic entity (120).

eIFs have also been investigated in the context of therapeutic strategies for lymphoma treatment. Mallya *et al.* could show that resistance to mTOR inhibition in a DLBCL cell line was caused by lack of 4E-BP1 expression, linking 4E-BP1 deficiency to lymphoma cell resistance to mTOR inhibition (121). Importantly, direct targeting of eIFs in lymphoma using inhibitor compounds has been shown to be of great promise (122-124). Silvestrol, for example, is a small molecule that inhibits translation initiation via modulation of eIF4A activity. It has been shown to enhance chemosensitivity in mouse lymphoma models driven, amongst others, by elevated eIF4E levels (124). Of note, silvestrol has also been reported to be effective against PIM kinase expressing lymphomas, which are especially drug-resistant (including Rapamycin resistance) and connected with worse patient outcome also in DLBCL. PIM signaling normally derepresses eIF4E, and, interestingly, directly inhibiting translation initiation via silvestrol in this study revealed to be even more effective than direct PIM kinase inhibitors (125). Moreover, there is evidence that eIF4A plays a particular role in the context of BCR activation in DLBCL, proposing once more the use of silvestrol for DLBCL

treatment (126). Another study by Culjkovic-Kraljacic *et al.* showed that high eIF4E expression was particularly associated with double- and triple-hit (DH/TH) DLBCLs with amplifications or translocations in *MYC* and *BCL2* and/or *BCL6*. Interestingly, eIF4E seems to drive not only translation of *MYC*, *BCL6* and *BCL2* mRNA, but also their nuclear export. Given this important role of eIF4E in DH/TH DLBCL, they tested inhibition of Hsp90, which maintains eIF4E activity, together with eIF4E inhibition by ribavirin in mouse models and detected more suppressed lymphoma growth than with either agent alone (127).

Table 2 shows an overview of studies investigating eIFs in DLBCL.

Table 2: A summary of studies investigating eIFs in DLBCL.

Investigated eIF	Investigated system	Detected effect	Literature source
eIF4B	DLBCL patient samples and cell lines	eIF4B is higher expressed in DLBCL compared to B-cell controls, what affects the translation of specific mRNAs involved in tumorigenesis; eIF4B is associated with worse patient outcome	Horvilleur *et al*. (119)
	DLBCL patient samples, cell lines and xenografts	FASN promotes oncogenic translation in DLBCL via eIF4B	Kapadia *et al.* (120)
eIF4E	DLBCL patient samples	eIF4E expression is associated with higher Ann Arbor Stages and inferior survival	Demosthenous *et al.*(112)
	DLBCL patient samples and cell lines	eIF4E overexpression compared to B-cell controls	Culjkovic *et al.* (113)
	DLBCL patient samples	phospho-eIF4E correlates with MCL-1 expression	Wendel *et al.* (108)
	DLBCL patient samples and cell lines	MNKs can modify oncogenic translation by regulating eIF4E1 and eIF4E3	Landon *et al.* (114)
	DLBCL patient samples, cell lines and xenografts	eIF4E is associated with DH/TH DLBCL	Culjkovic-Kraljacic *et al.* (127)
4E-BP1	DLBCL patient samples	Higher expression of 4E-BP1 compared to GCs of reactive lymphoid tissues	Kodali *et al.* (115)
	DLBCL patient samples	High levels of phospho-4E-BP1 are associated with worse patient outcome in low-risk DLBCL patients	Ninan *et al.* (116)
	DLBCL patient samples	High MYC expression is associated with increased 4E-BP1 phosphorylation	Pourdehnad *et al.* (117)
	DLBCL cell lines	Lack of 4E-BP1 expression is associated with resistance to mTOR inhibition	Mallya *et al.* (121)
eIF4GII	DLBCL patient samples, cell lines and xenografts	eIF4GII is a target of miR-520c-3p and higher expressed in DLBCL compared to B-cell controls	Mazan-Mamczarz *et al.* (118)

As described above, several studies have analyzed the role of eIFs in B-cell lymphoma and also in DLBCL. However, the focus was thereby primarily set on eIF4-factors. Therefore, a big range of eIFs has never been investigated in this neoplastic entity.

1.3 Aim of the thesis

Previous studies on some eIFs in lymphoma revealed that the translation initiation pathway is implicated in lymphomagenesis. However, data on the eIF expression pattern in DLBCL is limited. Therefore, the aim of this thesis was to shed light on the role of currently untested eIFs in DLBCL by performing an expression analysis in this aggressive B-cell lymphoma subtype. Thereby, the impact of certain eIFs on lymphomagenesis, their contribution to the disease-relevant DLBCL subtypes and also possible associations between eIF expression and patient survival were analyzed.

2 Material and Methods

The experiments for this study were performed with the following methods and using the referenced materials, as also described in Unterluggauer *et al.* (128).

2.1 Neoplastic patient samples

Neoplastic samples were collected at the Diagnostic and Research Institute of Pathology of the Medical University of Graz. In total, 56 DLBCL patient specimens were included in the study. Patients of the investigated local patient cohort received R-CHOP-like regimens, and the cohort had a median follow-up time of 5.7 years. Following the World Health Organization classification (129), 34 of the samples were primary DLBCL samples and 22 were secondary DLBCL samples originating from an FL grade 3. To determine the DLBCL subtype, the Hans algorithm (10) was applied using immunohistochemical stainings (see IHC section): Of the 34 primary DLBCL samples, 12 were classified as being of the GCB-DLBCL subtype and 19 as being of the nGCB-DLBCL subtype. Due to lacking tumor material, classification of three cases was not possible. Moreover, because secondary DLBCL arising from FL possesses an expression profile, which is similar to GCB-DLBCL (130), these cases were added to the GCB-DLBCL subtype for all analyses.

This retrospective study was approved by the ethics committee of the Medical University of Graz (Ethical application 28-040 ex 15/16).

2.2 Non-neoplastic controls

Using a FACS-ARIA3 cell sorter, non-neoplastic germinal center B-cells ($CD20^{high}$ and $CD38^{+}$) for quantitative real-time PCR (qRT-PCR) approaches were isolated, with informed consent, from five human tonsils collected from children and adolescents who underwent routine tonsillectomy. This procedure was approved by the local ethics committee of the Medical School of the University Duisburg-Essen (Ethical application 11-4799-30), and the following antibodies were used for this purpose: anti-CD20-antibody (Becton Dickinson, Franklin Lakes, NJ, USA; order number: 562873) and anti-CD38-antibody (Becton Dickinson; order number: 551400).

Furthermore, non-neoplastic human tonsils were collected for IHC analysis and qRT-PCR analysis. The respective tonsils were collected with informed consent from patients undergoing routine tonsillectomy, as approved by the ethics committee of the Medical University of Graz (Ethical application 28-040 ex 15/16).

2.3 RNA isolation and qRT-PCR

In general, fresh frozen cryo material was used for qRT-PCR investigations. Applying miRNeasy Mini Kit (Quiagen, Hilden, Germany) according to the manufacturer's instructions, RNA was extracted from DLBCL patient tissues as well as from non-neoplastic germinal center B-cells isolated by FACS cell sort. Transcription of isolated RNA into cDNA was performed by using the High Capacity cDNA Reverse Transcription Kit (Applied Biosystems, Foster City, CA, USA) according to the manufacturer's instructions. Finally, using a C1000 Touch Thermal Cycler CFX 384 Real-Time System (Bio-Rad Laboratories, Inc., Hercules, CA, USA), qRT-PCR was then performed in triplicate from produced cDNA according to the following protocol:

Reaction mix:
- 1x of GoTaq qPCR Master Mix (Promega, Madison, WI, USA)
- 0.1 µM of forward and reverse primer for detection of the respective gene (synthesized by Eurofins Genomics, Ebersberg, Germany)
- approximately 20 ng cDNA

Cycling protocol:
- Hot start activation (95°C for 2 min)
- 40 cycles of denaturation and annealing/extension (95°C for 15 s, 60°C for 30 s)
- Dissociation phase (60-95°C)

Table 3 shows the primer pairs used for qRT-PCR analysis.

Table 3: Oligonucleotide sequences of primers used for qRT-PCR analysis. Reproduced with modifications from (128). [http://creativecommons.org/licenses/by/4.0/]

Primer	Sequence (5'->3')
EIF1-f	GAAACGGCAGGAAGACCCTTA
EIF1-r	CGGATGCTCAATTACAGTACCAT
EIF1A-f	AACAGACGCAGGGGTAAGAAT
EIF1A-r	CCTGAGCATACTCCTGACCAT
EIF2A-f	GACCCCAACCATACAAGGTGG
EIF2A-r	TTCTCCATAGTAGGAAGCTCCTG
EIF2B3-f	GTGGAGGATCTCGGATGACAG
EIF2B3-r	GCTCAAGCAGGTTCAATGGGT
EIF2B4-f	CAGAGAACTGCCAGAATCGGG
EIF2B4-r	GTTCGGCCTTACTCCGACC
EIF2B5-f	TTCTGGTGGCCGATAGCTTC
EIF2B5-r	AGCTTTCCAGCAACAAAAGACA
EIF2S1-f	TGGTGAATGTCAGATCCATTGC
EIF2S1-r	TAGAACGGATACGCCTTCTGG
EIF3D-f	CAGCGGAATCGAATGAGATTTGC
EIF3D-r	GTTTGGCACTCTTAGGCAGGA
EIF3J-f	TGCCCACAATCCCTTGAACA
EIF3J-r	GGCAGCAAGATCCAAGTTCC
EIF3L-f	GGAGGAGATTGACTTTCTTCGTT
EIF3L-r	TTGGATTTGTCTACCAGGGAATG
EIF4A2-f	GAAGCCTTCCGCTATTCAGCA
EIF4A2-r	CTTGGGTCTCCTTGAACTCAATC
EIF4E-f	TGCGGCTGATCTCCAAGTTTG
EIF4E-r	CCCACATAGGCTCAATACCATC
EIF4EBP1-f	CACCCCGGGAGGTACCAGGATC
EIF4EBP1-r	CGCCCGCCCGCTTATCTTCT
EIF4G2-f	AGGGCAAAACGCTCAGAAATG
EIF4G2-r	TCCTGAAGATTGCATCATGTCG
EIF4G3-f	CCTAGAGCTACCATCCCGAAC
EIF4G3-r	GGGCCACTATGACGGTACTG
EIF5-f	AGCGTGTCAGACCAGTTCTAT
EIF5-r	CTGTCTTGATTCCATTGCCTTTG
ACTB-f	CTGGAACGGTGAAGGTGACA
ACTB-r	AAGGGACTTCCTGTAACAATGCA
GAPDH-f	AAGGTCGGAGTCAACGGATTT
GAPDH-r	ACCAGAGTTAAAAGCAGCCCTG

Actin and GAPDH were used as housekeeping genes. cDNA from non-neoplastic tonsils served as calibrator. Based on calculation $2^{-\Delta\Delta CT}$, the results are calculated as relative units. This gives the relative amount of the gene of interest normalized to the endogenous control (geometric mean of Actin and GAPDH) (131).

The qRT-PCR results were evaluated for each eIF: The results were evaluated regarding unusual melting patterns (e.g. double peak), the shape of amplification curves and standard deviation of triplicate CT values. If the pre-established criteria were not fulfilled, the respective specimens were excluded from all further analysis.

2.4 IHC staining

IHC analyses were performed to determine the subtype of DLBCL using the Hans algorithm (10) and also to analyze eIF expression in DLBCL as well as non-neoplastic tonsils at the protein level (eIF1A, eIF2B5, eIF3d).

For this purpose, stainings were performed according to the following protocol: Using Target Retrieval Solution (1:10, Dako, Glostrup, Denmark), formalin-fixed, paraffin-embedded material was pretreated in a water bath for 40 min (10 min 60°C, 30 min 100°C). Afterwards, slides were incubated with the primary antibody at room temperature for 30 min. The following primary antibodies were used to distinguish the DLBCL subtype: anti-CD10-antibody (1:6, Novocastra, Leica Biosystems, Wetzlar, Germany; order number: NCL-CD10-270), anti-MUM1-antibody (1:50, Dako; order number: M7259) and anti-BCL-6-antibody (1:100, Cell Marque, Rocklin, CA, USA; order number: 227M-96). In the case of anti-BCL-6-antibody, slides underwent a pretreatment phase with proteinase K (1:1500, Dako) for 10 min before primary antibody incubation. The following primary antibodies were used to analyze expression of eIFs at the protein level: anti-eIF1A-antibody (1:150, Abcam, Cambridge, United Kingdom; order number: ab177939), anti-eIF2B5-antibody (1:20, Santa Cruz Biotechnology, Dallas, TX, USA; order number: sc-55558) and anti-eIF3d-antibody (1:25, Santa Cruz Biotechnology; order number: sc-28856). For the staining process, the automated stainer intelliPATH FLX® (Biocare Medical, Pacheco, CA, USA) and kit K5001 (Dako) were used according to the manufacturer's instructions. As positive control, tissues

known to contain the respective antigens were used. As negative control, primary antibody was replaced with normal serum.

To evaluate staining intensity of eIFs, the following procedure was used: In case of DLBCL specimens, staining intensity of DLBCL cells, and in case of non-neoplastic tonsillar controls, staining intensity of germinal center centroblasts was evaluated. The scoring system ranged from score 0 to 3: Score 0 was assigned to no staining, score 1 to weak, score 2 to moderate and score 3 to strong staining intensity, respectively.

2.5 Cell culture

The lymphoma cell lines U-2932, Ri-1, KARPAS 422, SU-DHL-4, OCI-LY1 and NU-DUL-1 were grown in culture flasks in RPMI 1640 Medium (Gibco, Thermo Fisher Scientific, Waltham, MA, USA). Media were supplemented with 10% (U-2932, Ri-1, SU-DHL-4) or 20% (KARPAS 422, OCI-LY1, NU-DUL-1) Fetal Bovine Serum (Gibco, Thermo Fisher Scientific), respectively, and 1% Penicillin-Streptomycin (Gibco, Thermo Fisher Scientific). The immortalized B-cell line MUG-CC1-LCL was cultured with IMDM (Gibco, Thermo Fisher Scientific) and DMEM, high glucose (Gibco, Thermo Fisher Scientific) in a 1:1 mixture with 10% Fetal Bovine Serum. All cell lines were cultured at 37°C and with an atmosphere of 5% CO_2. To collect cell pellets, the cells were harvested by centrifugation. Afterwards, they were washed with DPBS (Gibco, Thermo Fisher Scientific) and stored at -80°C for further usage. The cell pellets of the immortalized B-cell line MUG-CC1-LCL were provided by the laboratory of Beate Rinner.

2.6 Protein isolation

Cell pellets were homogenized in Nonidet P 40 Substitute-based lysis buffer (0.05 M Tris-HCl, 0.15 M NaCl, 0.5% Nonidet P 40 Substitute (Sigma-Aldrich, Merck, Darmstadt, Germany), 0.1 mM Pefabloc SC (Roche, Basel, Switzerland), 1 mM DTT, cOmplete Tablets, Mini, EDTA-free (Roche) and PhosSTOP (Roche)) by repeatedly pipetting up and down. The lysate was then centrifuged at 4°C for 10 min at 10000 rpm. Using Bradford protein assay (Bio-Rad Laboratories, Inc.), the protein concentration of the resulting supernatant was determined, and the

samples were then taken up in SDS sample buffer (Bio-Rad Laboratories, Inc.) and subsequently stored at -80°C for further usage.

2.7 Western blot

Separation of protein samples according to their molecular mass was performed with SDS-PAGE (12.5% gel, Acrylamide/Bis Solution from Bio-Rad Laboratories, Inc.) and a vertical electrophoresis unit (Hoefer, Inc., Holliston, MA, USA). 25µg of protein was loaded onto the gels. Afterwards, using a Semi-Dry Blotter (Scie-Plas Ltd., Cambourne, United Kingdom), the proteins were transferred onto a PVDF-membrane (Immobilon-P Transfer Membrane, Merck Millipore, Merck). To avoid unspecific binding during immunodetection, the membrane was blocked using 5% nonfat dried milk powder (AppliChem GmbH, Darmstadt, Germany) in 0.1% TBS-Tween (Tween 20 from Merck Millipore, Merck) for 1 hour. After blocking, the membrane was washed with 0.1% TBS-Tween and then incubated with the primary antibody, agitating overnight at 4°C. Subsequently, the membrane was washed again with 0.1% TBS-Tween and then incubated with the secondary antibody for 1 hour. After another washing step with 0.1% TBS-Tween, the membrane signal was detected with Amersham ECL Prime/Select Western Blotting Detection Reagent (GE Healthcare, Chicago, IL, USA) and exposure to the detector ImageQuant LAS 500 (GE Healthcare). Actin was used as a loading control.

The following primary antibodies were used for eIF Western blot analyses: Anti-eIF1A-antibody (1:10000, Abcam; order number: ab177939), anti-eIF2α-antibody (1:1000, Cell Signaling Technology, Danvers, MA, USA; order number: 5324), anti-phospho-eIF2α-antibody (1:1000, Cell Signaling Technology; order number: 3398), anti-eIF3d-antibody (1:1000, Santa Cruz; order number: sc-28856), anti-eIF4E-antibody (1:1000, Cell Signaling Technology; order number: 9742), anti-4E-BP1-antibody (1:1000, Cell Signaling Technology; order number: 9452), anti-phospho-4E-BP1-antibody (1:1000, Cell Signaling Technology, order number: 9456), and anti-Actin-antibody (1:2000, Sigma-Aldrich, Merck; order number: A2103). The primary antibody was diluted using 5% Bovine Serum Albumin Fraction V (Roche) in 0.1% TBS-Tween. Amersham ECL Rabbit IgG (1:5000, GE Healthcare; order number: NA934-1ML) served as secondary antibody. Dilution of

the secondary antibody was performed using 5% milk powder in 0.1% TBS-Tween.

2.8 Statistical comparison of eIF expression levels in DLBCL and B-cell controls

To perform eIF expression analysis using qRT-PCR and IHC data, IBM SPSS Statistics for Windows, Version 23.0 (IBM Corp., Armonk, NY, USA), and GraphPad Prism, Version 5.01 for Windows (GraphPad Software, Inc., La Jolla, CA, USA) were used.

To test the mRNA data for normality of distribution within the different groups tested, the Shapiro Wilk test was used. Depending on the test result, a t-test was used afterwards, or a Mann-Whitney test was performed as non-parametric counterpart: Expression of eIFs at the mRNA level was thereby compared between non-neoplastic germinal center B-cells, DLBCL and its respective subtypes in an explorative manner.

In case of IHC analysis, differences in eIF expression between non-neoplastic germinal center centroblasts, DLBCL and its respective subtypes were investigated using Fisher's exact test.

2.9 Univariate survival analysis

To investigate possible prognostic impact of eIF expression in an explorative manner, patient survival in the study cohort as well as in two external mRNA expression data sets was analyzed. Due to the lack of follow-up data, two patients of the study cohort had to be excluded from the analysis. The mRNA expression data sets published by Shipp *et al.* (132) (n=58) and Lenz *et al.* (47) (n=200) were used as external cohorts.

To stratify potential risk groups based on the mRNA data, patients in all three cohorts investigated were subdivided into two groups using the 3rd quartile of the respective eIF expression levels within the cohort. Similarly, when analysing the IHC data of the study cohort regarding patient survival, patients with the highest score (score 3) were opposed to the rest.

To perform univariate survival analysis, IBM SPSS Statistics for Windows, Version 23.0 (IBM Corp.) was used. Kaplan-Meier plots were thereby applied to depict survival outcome. The log-rank test was used to statistically evaluate differential survival.

2.10 Multivariate survival analysis

The Cox proportional hazards model was used to investigate patient survival in the study cohort in relation to *EIF2B5* mRNA levels while adjusting for other potential nuisance factors. IBM SPSS Statistics for Windows, Version 23.0 (IBM Corp.), and R Version 3.4.1 (133) implementing the R-packages “survival” and “survminer” were used, and it was corrected for the following covariates: “Sex” (female vs male), “age” (continuous), “Ann Arbor Stage” (stage I+II vs stage III+IV) and “DLBCL subtype” (GCB- vs nGCB-DLBCL). Applicability of the Cox proportional hazards model was tested by checking for the proportional hazards assumption, as well as for the linearity of the continuous covariate “age” and for outliers by Schönfeld, Martingale and Deviance residuals. Besides multivariate analysis, univariate analysis of the variables was also performed.

3 Results

The following chapters are dedicated to the results of this study and their discussion, which have largely also been published in Unterluggauer *et al.* (128).

3.1 A comprehensive mRNA expression profile of eIFs shows dramatically dysregulated translation initiation in DLBCL

3.1.1 Study set-up and patient cohort

To exploratively investigate the role of eIFs in lymphomagenesis, a DLBCL sample cohort of 56 DLBCL patients was analyzed by qRT-PCR for the mRNA expression profile of 16 eIFs.

The patient cohort consisted of 34 primary DLBCL cases and 22 secondary DLBCL cases, originating from an FL grade 3 (**Table 4**). Using the Hans classification (10), the patient cohort could be separated into 34 GCB-DLBCLs and 19 nGCB-DLBCLs (see also **Material and Methods**). The 22 secondary DLBCL cases were thereby all added to the GCB-DLBCL subtype, yielding the secondary GCB-DLBCL subtype in contrast to the primary GCB-DLBCL subtype. Three cases were not classifiable because of lacking tumor material.

As controls, germinal center B-cells were purified from non-neoplastic tonsils of 5 patients, who underwent routine tonsillectomy, to compare their eIF expression profile with that of the DLBCL samples.

The eIFs, investigated at the mRNA level, were as follows: *EIF1*, *EIF1A*, *EIF2A*, *EIF2B3*, *EIF2B4*, *EIF2B5*, *EIF2S1*, *EIF3D*, *EIF3J*, *EIF3L*, *EIF4A2*, *EIF4E*, *EIF4EBP1*, *EIF4G2*, *EIF4G3*, and *EIF5*. They contribute to various steps of the translation initiation pathway and can be principally separated into two groups: *EIF2A*, *EIF2B3*, *EIF2B4*, *EIF2B5*, *EIF2S1*, *EIF5*, *EIF3D*, *EIF3J* and *EIF3L* are primarily engaged at the beginning of the translation initiation pathway (see schematic pathway in **Figure 7** and **Figure 8**) (52, 58, 79, 134). *EIF1*, *EIF1A*, *EIF4A2*, *EIF4E*, *EIF4EBP1*, *EIF4G2*, and *EIF4G3*, in contrast, primarily find their place later on during translation initiation (see schematic pathway in **Figure 9** and **Figure 10**) (52, 57, 135, 136).

Table 4: Patient characteristics of the study cohort. Percentage within the cohort was calculated by dividing the number of patients with the indicated parameter characteristic by the number of patients with information about this clinicopathologic parameter. Partly built upon (128). [http://creativecommons.org/licenses/by/4.0/]

Clinicopathologic parameter	Proportion within the study cohort
Gender	
Female	28/56 (50%)
Male	28/56 (50%)
Age at diagnosis	
<60 years	12/56 (21%)
>60 years	44/56 (79%)
Ann Arbor Stage	
Stage I	9/55 (16%)
Stage II	12/55 (22%)
Stage III	18/55 (33%)
Stage IV	16/55 (29%)
IPI (IPI score)	
Low (0-1)	15/54 (28%)
Intermediate (2-3)	27/54 (50%)
High (4-5)	12/54 (22%)
DLBCL subtype according to the Hans algorithm	
GCB	34/53 (64%)
pGCB	12/34 (35%)
sGCB	22/34 (65%)
nGCB	19/53 (36%)

Abbreviations: GCB-DLBCL (GCB), primary GCB-DLBCL (pGCB), secondary GCB-DLBCL originating from an FL grade 3 (sGCB), nGCB-DLBCL (nGCB).

3.1.2 Most of the eIFs tested show higher expression in DLBCL in comparison to non-neoplastic controls

According to the separation stated above, the mRNA expression results of the eIFs tested were summarized into eIFs involved in early steps of the translation initiation pathway and eIFs involved in later steps of the translation initiation pathway. Furthermore, the eIFs were grouped according to their function, yielding the four functionally interrelated groups “eIF2-cycle and eIF2A”, “eIF3-subunits”, “eIF1 and eIF1A”, and “eIF4-factors”.

3.1.2.1 eIFs involved in early steps of the translation initiation pathway

Regarding the eIF2-cycle, the mRNA levels of eIF2α (mRNA: *EIF2S1*), three subunits of eIF2B and eIF5 were analyzed (78). Furthermore, the mRNA expression profile of eIF2A, an alternative tRNAi-carrier (134), was also investigated (see **Figure 7**). All eIFs tested, involved in the eIF2-cycle, revealed higher mRNA expression in DLBCL when compared to non-neoplastic controls ($p<0.002$). Interestingly, *EIF2A* revealed a different picture. It did not show a considerably higher expression in DLBCL as a whole and even a lower expression in one of the DLBCL subtypes, the primary GCB-DLBCL subtype, in comparison to non-neoplastic germinal center B-cells ($p<0.04$).

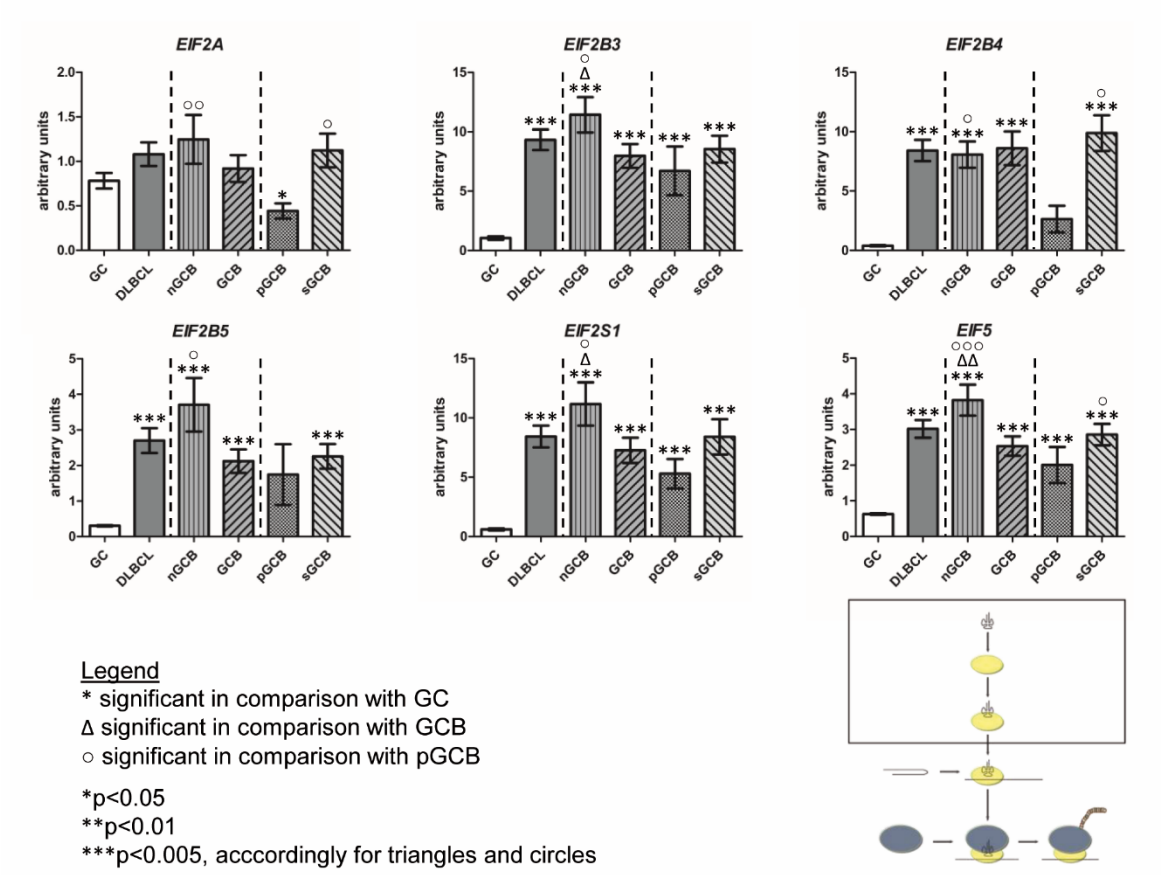

Figure 7: Expression analysis on the mRNA level: eIF2-cycle and eIF2A. The subtype-specific eIF mRNA expression profile in DLBCL was determined by qRT-PCR and compared within DLBCL and additionally with that of non-neoplastic germinal center B-cells. In the figure relative mRNA levels are depicted. Each bar shows the mean +/- standard error of the mean. Comparison was drawn between non-neoplastic germinal center B-cells (GC) and DLBCL, separated into the subtypes nGCB-DLBCL (nGCB) and GCB-DLBCL (GCB). Further distinction was made within the GCB-DLBCL subtype by distinguishing primary GCB-DLBCL (pGCB) from secondary GCB-DLBCL originating from an FL grade 3 (sGCB). Schematic pathway in the right corner illustrates involvement of depicted eIFs in early steps of the translation initiation pathway. Reproduced with modifications from (128). [http://creativecommons.org/licenses/by/4.0/]

Three eIF3-subunits were investigated regarding their mRNA expression profile in DLBCL (**Figure 8**). Importantly, *EIF3J* and *EIF3L* did not show considerably higher expression in DLBCL when compared to non-neoplastic germinal center B-cells. However, *EIF3D* was strongly overexpressed in DLBCL in comparison to non-neoplastic controls ($p<0.001$).

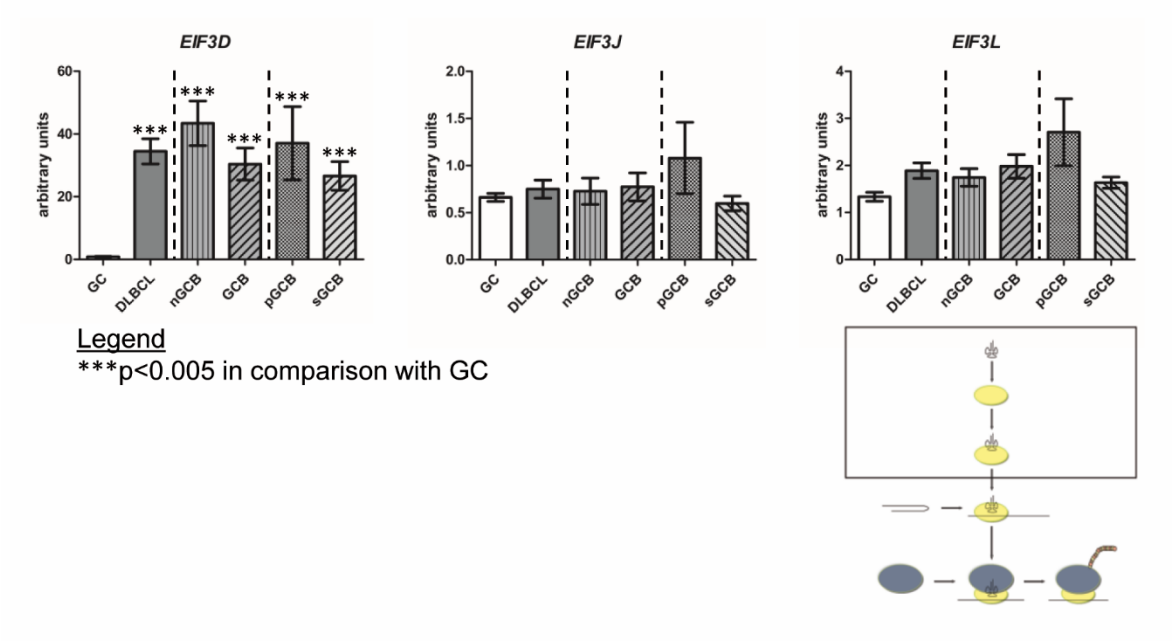

Figure 8: Expression analysis on the mRNA level: eIF3-subunits. The subtype-specific eIF mRNA expression profile in DLBCL was determined by qRT-PCR and compared within DLBCL and additionally with that of non-neoplastic germinal center B-cells. In the figure relative mRNA levels are depicted. Each bar shows the mean +/- standard error of the mean. Comparison was drawn between non-neoplastic germinal center B-cells (GC) and DLBCL, separated into the subtypes nGCB-DLBCL (nGCB) and GCB-DLBCL (GCB). Further distinction was made within the GCB-DLBCL subtype by distinguishing primary GCB-DLBCL (pGCB) from secondary GCB-DLBCL originating from an FL grade 3 (sGCB). Schematic pathway in the right corner illustrates involvement of depicted eIFs in early steps of the translation initiation pathway. Reproduced with modifications from (128). [http://creativecommons.org/licenses/by/4.0/]

3.1.2.2 eIFs involved in later steps of the translation initiation pathway

The factors eIF1 and eIF1A are especially important for start codon scanning during translation initiation (58). Compared to non-neoplastic germinal center B-cells, the mRNA expression profile of *EIF1* and *EIF1A* showed overexpression in DLBCL ($p<0.001$, **Figure 9**).

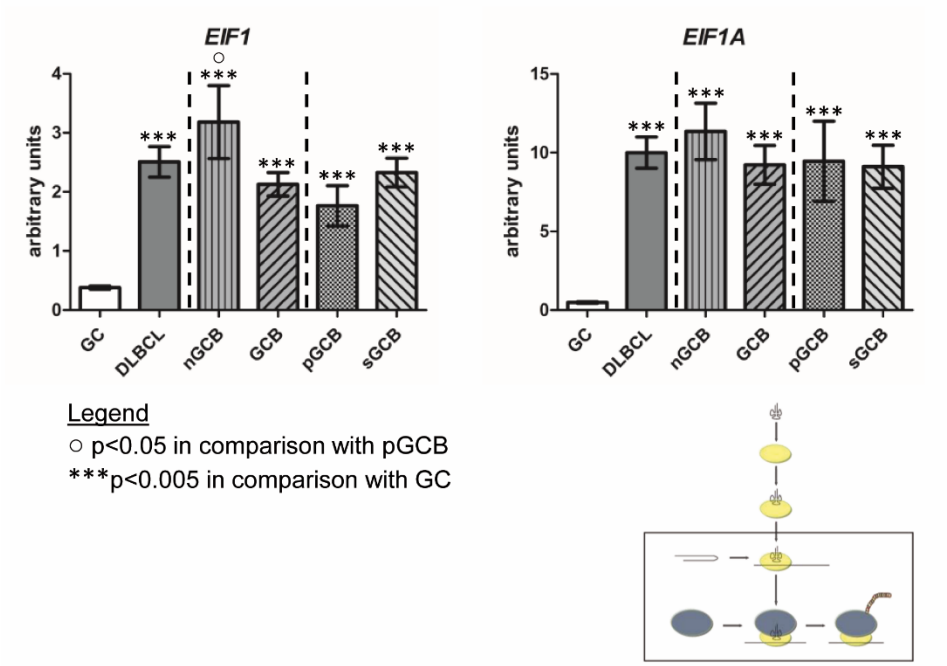

Figure 9: Expression analysis on the mRNA level: eIF1 and eIF1A. The subtype-specific eIF mRNA expression profile in DLBCL was determined by qRT-PCR and compared within DLBCL and additionally with that of non-neoplastic germinal center B-cells. In the figure relative mRNA levels are depicted. Each bar shows the mean +/- standard error of the mean. Comparison was drawn between non-neoplastic germinal center B-cells (GC) and DLBCL, separated into the subtypes nGCB-DLBCL (nGCB) and GCB-DLBCL (GCB). Further distinction was made within the GCB-DLBCL subtype by distinguishing primary GCB-DLBCL (pGCB) from secondary GCB-DLBCL originating from an FL grade 3 (sGCB). Schematic pathway in the right corner illustrates involvement of depicted eIFs in later steps of the translation initiation pathway. Reproduced with modifications from (128). [http://creativecommons.org/licenses/by/4.0/]

All five eIF4-factors tested participate in mRNA recruitment to the ribosome *(57, 136)*. *EIF4A2*, *EIF4E*, *EIF4EBP1* and *EIF4G2* (alternative name: *DAP5*) showed increased mRNA expression in DLBCL when compared to non-neoplastic controls ($p<0.003$, **Figure 10**). In contrast, only *EIF4G3* (alternative name: *EIF4GII*), only one of five eIF4-factors tested, did not reveal considerable mRNA overexpression in DLBCL.

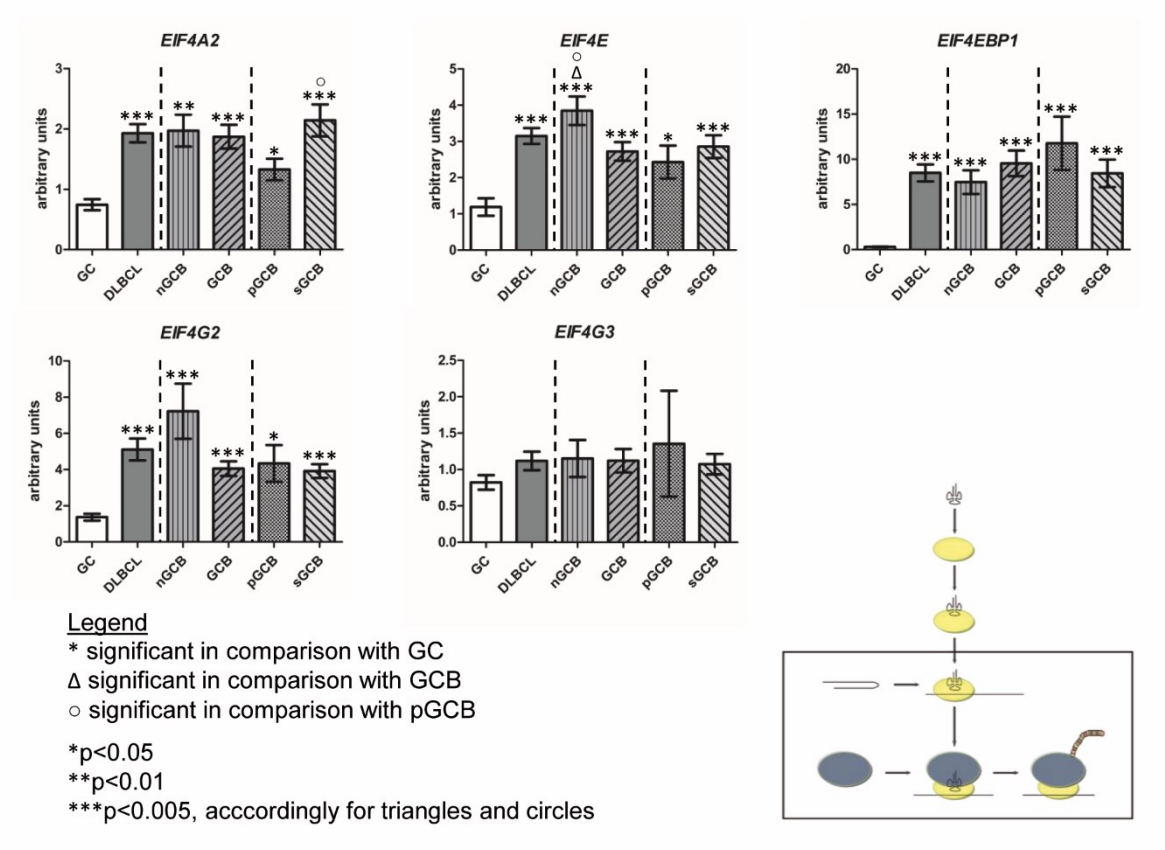

Figure 10: Expression analysis on the mRNA level: eIF4-factors. The subtype-specific eIF mRNA expression profile in DLBCL was determined by qRT-PCR and compared within DLBCL and additionally with that of non-neoplastic germinal center B-cells. In the figure relative mRNA levels are depicted. Each bar shows the mean +/- standard error of the mean. Comparison was drawn between non-neoplastic germinal center B-cells (GC) and DLBCL, separated into the subtypes nGCB-DLBCL (nGCB) and GCB-DLBCL (GCB). Further distinction was made within the GCB-DLBCL subtype by distinguishing primary GCB-DLBCL (pGCB) from secondary GCB-DLBCL originating from an FL grade 3 (sGCB). An alternative name for *EIF4G2* is *DAP5*, an alternative name for *EIF4G3* is *EIF4GII*. Schematic pathway in the right corner illustrates involvement of depicted eIFs in later steps of the translation initiation pathway. Reproduced with modifications from (128). [http://creativecommons.org/licenses/by/4.0/]

Thus, 12 out of 16 eIFs tested revealed a higher mRNA expression in DLBCL when compared to non-neoplastic germinal center B-cells ($p<0.003$, **Figure 7**, **Figure 8**, **Figure 9** and **Figure 10**). The result was thereby independent from whether an eIF acted at the first steps of translation initiation or later on in the pathway. In both groups, most of the eIFs were overexpressed in DLBCL. There were only 4 eIFs that did not show a considerable overexpression in DLBCL:

EIF2A, *EIF3J*, *EIF3L*, and *EIF4G3*. Of note, among these eIFs, there were two of the three eIF3-subunits tested.

3.1.3 Selected eIFs are higher expressed in nGCB-DLBCL in comparison to GCB-DLBCL

In addition to the comparison with non-neoplastic germinal center B-cells, eIF mRNA expression in DLBCL was also exploratively investigated regarding the disease-relevant DLBCL subtypes.

The subtype-specific analysis revealed for 8 of the 16 eIFs investigated a considerably higher mRNA expression in the nGCB-DLBCL subtype in comparison with the GCB-DLBCL subtype (see **Figure 7**, **Figure 9** and **Figure 10**). These eIFs were as follows: *EIF1*, *EIF2A*, *EIF2S1*, *EIF2B3*, *EIF2B4*, *EIF2B5*, *EIF4E*, and *EIF5* (in comparison with both GCB-DLBCL subtypes and the primary/secondary GCB-DLBCL subtype alone: $p<0.05$). Particularly noteworthy, *EIF2B5* and *EIF5* were twofold and 1.5-fold higher expressed in the nGCB-DLBCL subtype, respectively (compared to both GCB-DLBCL subtypes: $p=0.058$ and $p=0.007$, respectively; compared to the primary GCB-DLBCL subtype alone: $p=0.043$ and $p=0.001$, respectively).

As stated above, the GCB-DLBCL group consisted of primary GCB-DLBCLs and secondary GCB-DLBCLs (originating from an FL grade 3). Interestingly, the majority of eIFs tended to be expressed more strongly in the secondary GCB-DLBCL subtype when compared to the primary one, which was most pronounced for *EIF2A*, *EIF2B4*, *EIF4A2* and *EIF5* ($p<0.03$, **Figure 7** and **Figure 10**).

The results of the performed explorative mRNA expression analysis of the study cohort, thus, pointed towards a strongly dysregulated translation initiation pathway in DLBCL. Interestingly, the mRNA data not only indicated that most eIFs tested were overexpressed in DLBCL, but also that some selected ones showed higher expression in the nGCB-DLBCL subtype than in the GCB-DLBCL subtype. However, it is the protein level which in general reflects the effector state of an mRNA.

Accordingly, based on the remarkable expression profile, three eIFs were chosen to be tested for confirmation by IHC: eIF1A, eIF2B5, and eIF3d. All 3 showed

particularly interesting mRNA results (see above): Expression of *EIF1A*, *EIF2B5*, and *EIF3D* was 8- to 40-fold higher in DLBCL than in non-neoplastic controls. Furthermore, the expression of *EIF2B5* was twofold higher in the nGCB-DLBCL subtype than in the (p)GCB-DLBCL subtype.

3.2 Validation of the mRNA expression analysis on the protein level

3.2.1 IHC confirms eIF1A and eIF3d overexpression in DLBCL

By comparing DLBCL with non-neoplastic germinal center B-cell controls, *EIF1A* and *EIF3D* revealed a remarkably higher mRNA expression in DLBCL. To confirm mRNA data on the protein level, immunohistochemical analyses for both eIFs were performed. Therefore, 22 primary and secondary DLBCL specimens of the study cohort were stained with an antibody against the respective proteins eIF1A and eIF3d. Additionally, 10 non-neoplastic tonsil specimens of patients undergoing routine tonsillectomy were used as controls. The eIF1A and eIF3d staining intensities of DLBCL cells were then compared with the respective staining intensities of germinal center centroblasts of non-neoplastic tonsils.

As shown in **Figure 11**, the DLBCL specimens exhibited a homogeneous cytoplasmic staining of eIF1A and eIF3d.

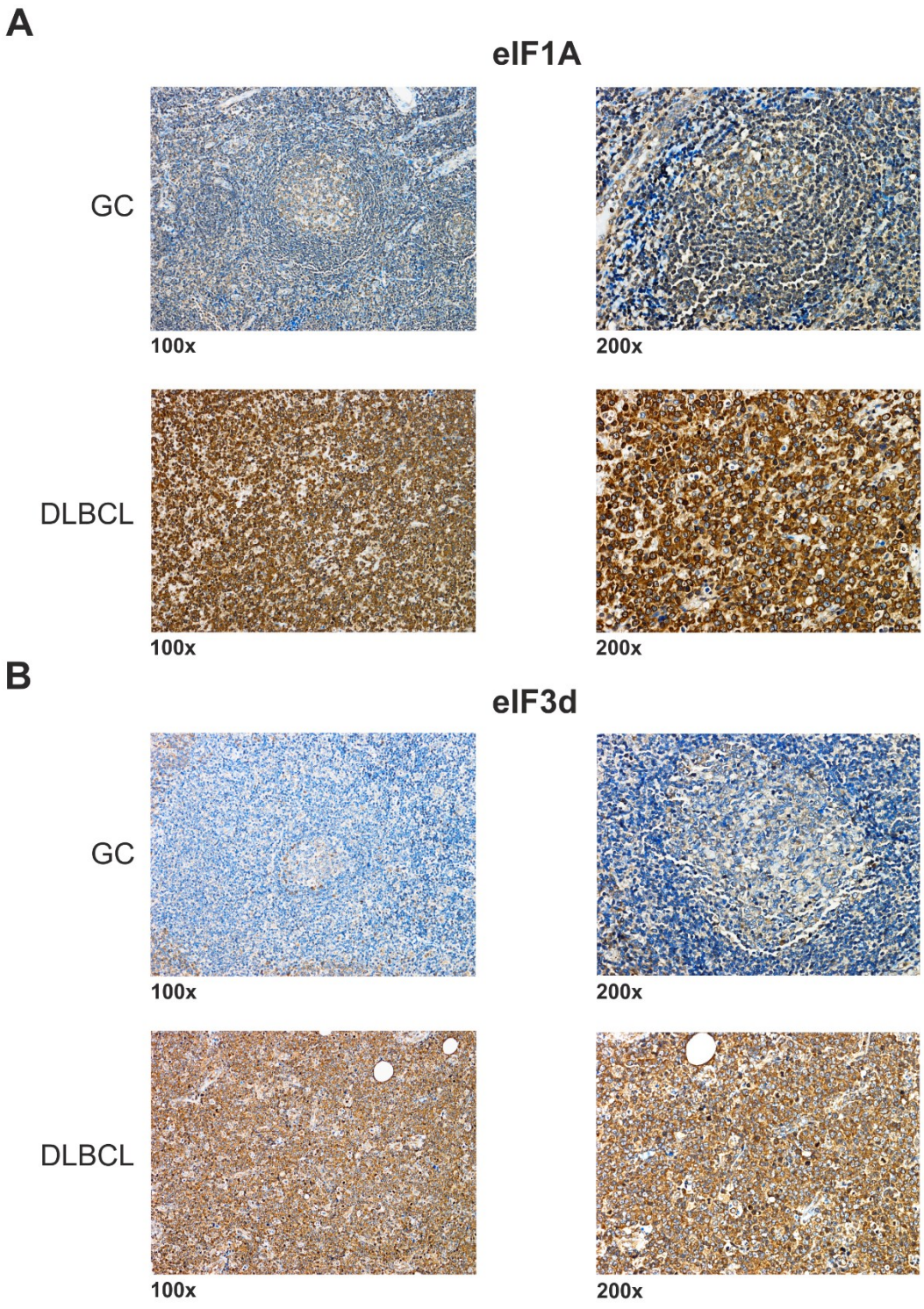

Figure 11: Analysis of eIF1A and eIF3d protein expression in non-neoplastic tonsillar germinal centers and DLBCL specimens using immunohistochemical stainings – Representative staining results. The expression of eIF1A (**A**) and eIF3d (**B**) in tonsillar germinal centers (GC) and DLBCL is depicted by representative immunohistochemical staining examples (with 100x and 200x magnification). Images were captured by the use of an Olympus BX51 microscope and an Olympus E-330 camera. Reproduced with modifications from (128). [http://creativecommons.org/licenses/by/4.0/]

Importantly, the DLBCL specimens furthermore revealed stronger staining intensities than the germinal center centroblasts of non-neoplastic tonsils also tested (p=0.048 for eIF1A, p=0.015 for eIF3d, **Figure 11**, **Figure 12**, **Table 5**). This implied overexpression of eIF1A and eIF3d in DLBCL also on the protein level confirming mRNA data.

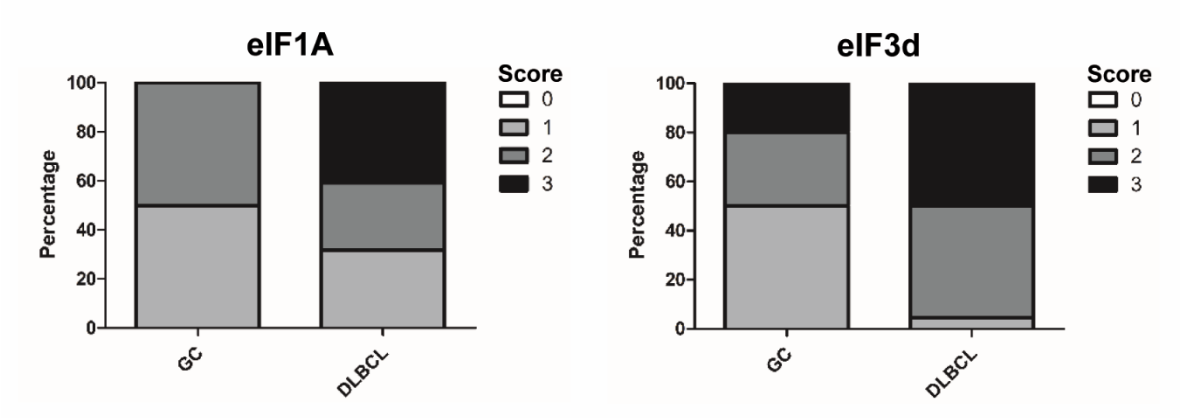

Figure 12: Analysis of eIF1A and eIF3d protein expression in non-neoplastic tonsillar germinal centers and DLBCL specimens using immunohistochemical stainings – Scoring results. The expression profile of eIF1A and eIF3d in tonsillar germinal center centroblasts (GC) and DLBCL is depicted in a graphical representation summarizing all staining intensities. Staining intensities were evaluated with a scoring system from 0 to 3. Reproduced with modifications from (128). [http://creativecommons.org/licenses/by/4.0/]

Table 5: Immunohistochemical analysis of eIF1A and eIF3d expression of non-neoplastic tonsillar germinal center centroblasts (GC) in comparison with DLBCL cells. Staining intensities were evaluated with a scoring system from 0 to 3. Reproduced with modifications from (128). [http://creativecommons.org/licenses/by/4.0/]

	0 (-)	1 (+)	2 (++)	3 (+++)	p-value
eIF1A					
GC	0/10	5/10	5/10	0/10	
DLBCL	0/22	7/22	6/22	9/22	0.048[a]
eIF3d					
GC	0/10	5/10	3/10	2/10	
DLBCL	0/22	1/22	10/22	11/22	0.015[a]

[a]$p<0.05$ compared to GC

3.2.2 IHC confirms eIF2B5 overexpression in DLBCL and its higher expression in the nGCB-DLBCL subtype

Similarly to *EIF1A* and *EIF3D*, *EIF2B5* also exhibited higher mRNA expression in DLBCL compared to non-neoplastic germinal center B-cells, and importantly, it additionally showed a higher expression in the nGCB-DLBCL subtype than in the GCB-DLBCL subtype. To confirm this observation on the protein level, 49 primary and secondary DLBCL specimens of the study cohort were immunohistochemically analyzed. Again, 10 non-neoplastic tonsil specimens from routine tonsillectomies served as controls.

The DLBCL specimens exhibited a homogeneous cytoplasmic staining of eIF2B5 (see **Figure 13**). Furthermore, as for eIF1A and eIF3d, IHC analysis confirmed the mRNA overexpression of *EIF2B5* in DLBCL also on the protein level. DLBCL specimens revealed stronger eIF2B5 staining intensities than the control non-neoplastic tonsillar germinal center centroblasts ($p<0.001$, **Figure 13**, **Figure 14**, **Table 6**).

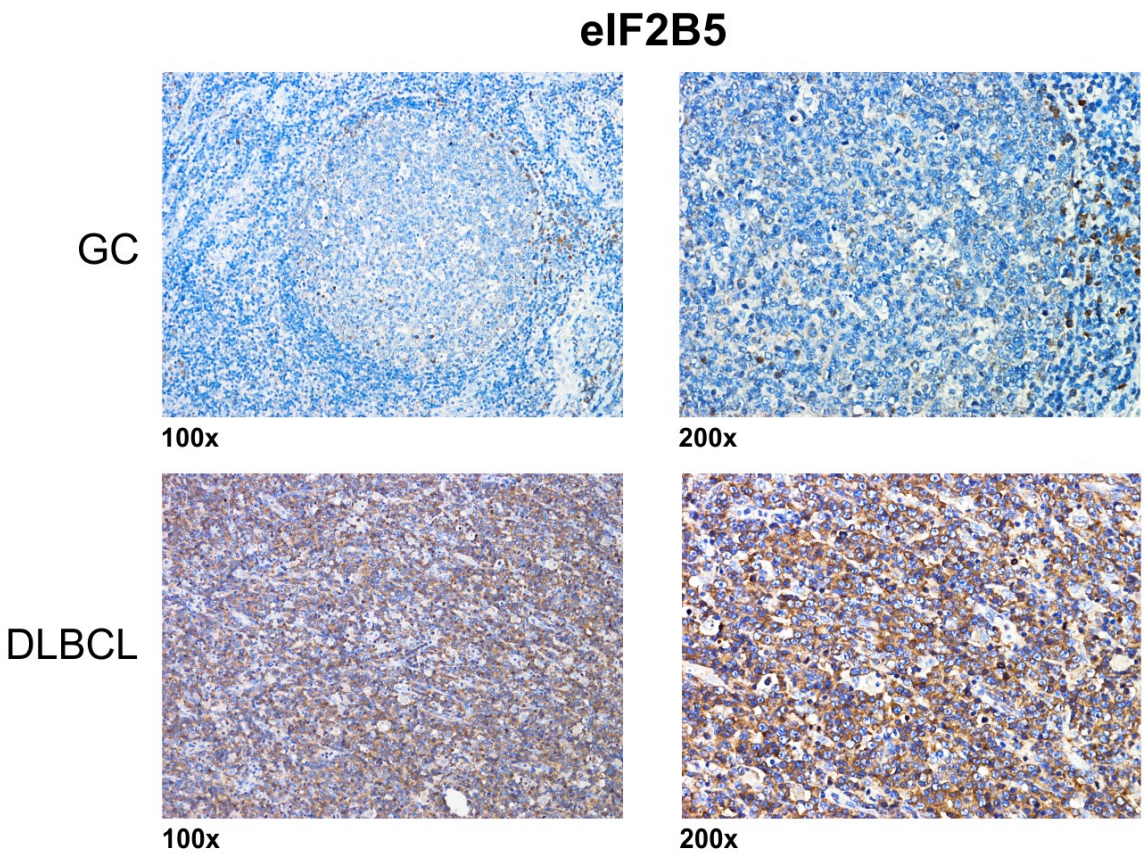

Figure 13: Analysis of eIF2B5 protein expression in non-neoplastic tonsillar germinal centers and DLBCL specimens using immunohistochemical stainings – Representative staining results. The expression of eIF2B5 in tonsillar germinal centers (GC) and DLBCL is depicted by representative immunohistochemical staining examples (with 100x and 200x magnification), Images were captured by the use of an Olympus BX51 microscope and an Olympus E-330 camera. Reproduced with modifications from (128). [http://creativecommons.org/licenses/by/4.0/]

To analyze also the subtype-specific eIF2B5 expression on the protein level, we compared the immunohistochemical eIF2B5 staining pattern of all DLBCL specimens with available subtype classification (nGCB-DLBCL n = 18, primary GCB-DLBCL n = 9, secondary GCB-DLBCL n = 20). This analysis also confirmed the mRNA data, revealing eIF2B5 staining intensities in the nGCB-DLBCL subtype that were stronger than those in the GCB-DLBCL subtype (p=0.038, **Figure 14**, **Table 6**).

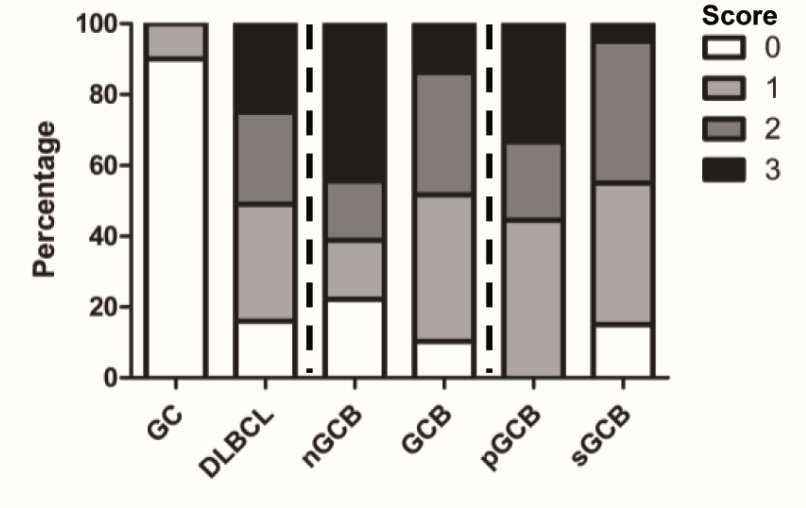

Figure 14: Analysis of eIF2B5 protein expression in non-neoplastic tonsillar germinal centers and DLBCL specimens using immunohistochemical stainings – Scoring results. The expression profile of eIF2B5 in tonsillar germinal center centroblasts (GC) and DLBCL is depicted in a graphical representation summarizing all staining intensities. Staining intensities were evaluated with a scoring system from 0 to 3. Abbreviations: nGCB-DLBCL (nGCB), GCB-DLBCL (GCB), primary GCB-DLBCL (pGCB), secondary GCB-DLBCL originating from an FL grade 3 (sGCB). Reproduced with modifications from (128). [http://creativecommons.org/licenses/by/4.0/]

Table 6: Immunohistochemical analysis of eIF2B5 expression of non-neoplastic tonsillar germinal center centroblasts (GC) in comparison with DLBCL cells. Staining intensities were evaluated with a scoring system from 0 to 3. Reproduced with modifications from (128). [http://creativecommons.org/licenses/by/4.0/]

eIF2B5	0 (-)	1 (+)	2 (++)	3 (+++)	p-value
GC	9/10	1/10	0/10	0/10	
DLBCL					<0.001[a]
nGCB	4/18	3/18	3/18	8/18	0.003[a]
GCB (pGCB+sGCB)	3/29	12/29	10/29	4/29	<0.001[a], 0.038[b]
pGCB	0/9	4/9	2/9	3/9	<0.001[a]
sGCB	3/20	8/20	8/20	1/20	<0.001[a], 0.017[b]

Abbreviations: nGCB-DLBCL (nGCB), GCB-DLBCL (GCB), primary GCB-DLBCL (pGCB), secondary GCB-DLBCL originating from an FL grade 3 (sGCB).
[a] $p<0.05$ vs GC
[b] $p<0.05$ vs nGCB

Summing up, IHC analyses could thus confirm the mRNA data of eIF1A, eIF3d and eIF2B5 on the protein level.

3.2.3 Additional confirmation of mRNA data by Western blot analysis

To validate the mRNA data on the protein level also with a second method, eIF expression was investigated in DLBCL cell lines and a control B-cell line by Western blot analysis. For this aim, pellets of 6 different DLBCL cell lines (Ri-1, U-2932, NU-DUL-1, SU-DHL-4, KARPAS 422 and OCI-LY1) and an immortalized non-neoplastic B-cell line (MUG-CC1-LCL) were harvested, cells lysed and the lysates applied to immunoblot analysis. Membranes were probed for those eIFs of the mRNA analysis, for which established antibodies for Western blot detection were already available in our laboratory: eIF1A, eIF2α, eIF3d, eIF4E and 4E-BP1.

Regarding eIF3d and eIF4E, all DLBCL cell lines showed considerably stronger expression than the immortalized non-neoplastic B-cell line (**Figure 15**). The expression profile of eIF1A and 4E-BP1 revealed, in contrast, more variation, but

also here most lymphoma cell lines exhibited a clearly stronger expression of both eIFs than the immortalized non-neoplastic B-cell line. Finally, also for eIF2α, expression in DLBCL cell lines was stronger than in the B-cell line, although the expression intensity between lymphoma cell lines and B-cell line did not differ as much as in the case of the other eIFs tested.

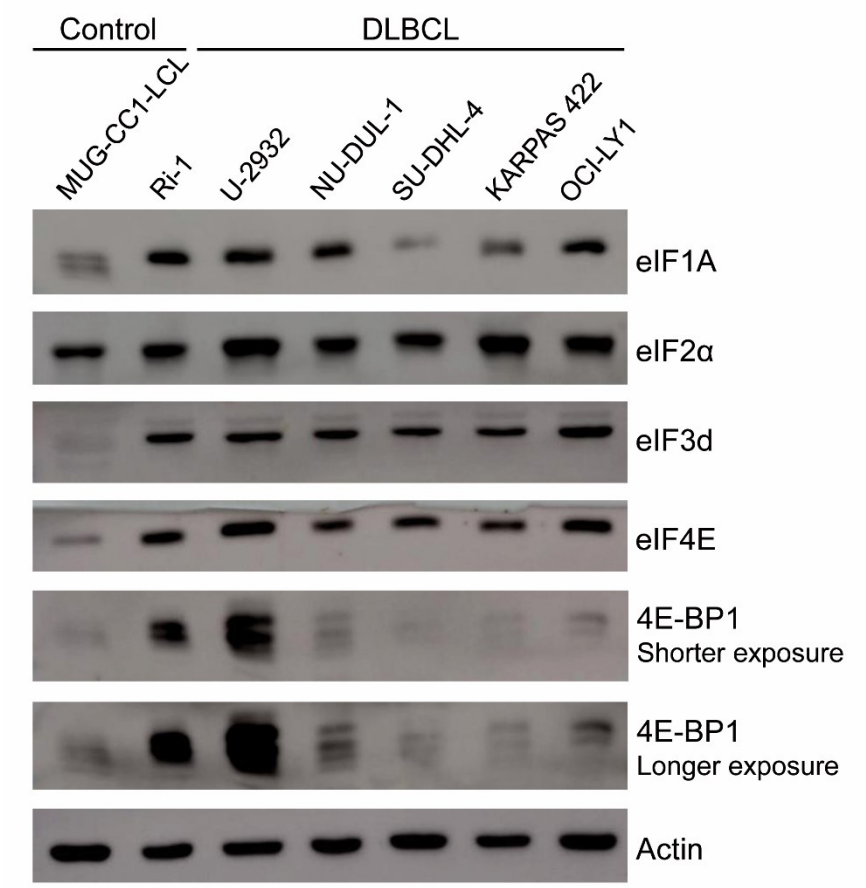

Figure 15: Western blot analysis of eIF expression in DLBCL cell lines (DLBCL) and a control B-cell line (Control). Actin was used as a loading control. Signals were detected and images were taken using the ImageQuant LAS 500.

Thus, since all of these eIFs also showed overexpression in DLBCL in the mRNA analysis, the Western blot analysis confirmed the corresponding mRNA data on the protein level. Importantly, the higher expression of eIF1A and eIF3d in DLBCL in comparison to non-neoplastic controls could therefore be demonstrated by qRT-PCR and IHC using patient samples, as well as by Western blot using cell lines.

Furthermore, already established antibodies for the detection of phospho-eIF2α and phospho-4E-BP1 allowed for the analysis of the phosphorylation status of eIF2α and 4E-BP1 in DLBCL cell lines in comparison to the control B-cell line. As already stated above, phosphorylation of these two eIFs occurs in the context of associated upstream signaling pathways, which regulate translation, and is also a matter of cancer research (58, 62). Regarding the phosphorylation status, no essential difference was visible, because when considering the basal expression levels of the two factors, the phosphorylation status of eIF2α and 4E-BP1 was similar between lymphoma cell lines and B-cell line (**Figure 16**).

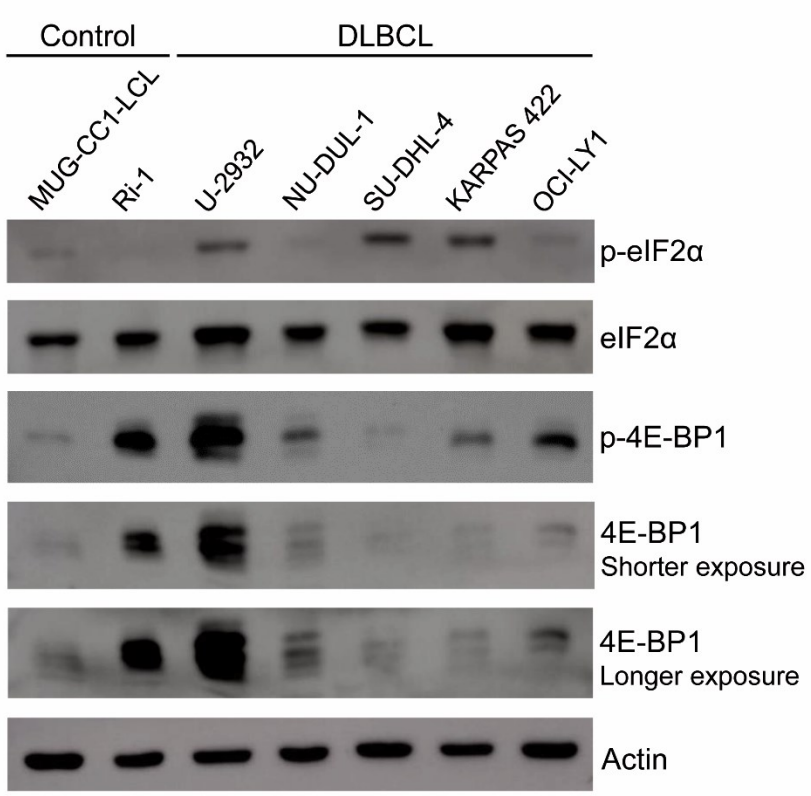

Figure 16: Western blot analysis of phospho-eIF2α (p-eIF2α) and phospho-4E-BP1 (p-4E-BP1) in DLBCL cell lines (DLBCL) and a control B-cell line (Control). Actin was used as a loading control. Signals were detected and images were taken using the ImageQuant LAS 500.

To repeat the Western blot analysis, the cell lines were kept in culture and again pellets were taken a few weeks after the first pellet collection. The results of the following immunoblot detection are depicted in **Figure 17**. Taking into account the Actin band, there was in general again a higher expression of eIF1A, eIF2α, eIF3d, eIF4E and 4E-BP1 in the DLBCL cell lines in comparison with the control B-cell line (**Figure 17A**), although in most cases the differences were not as big as in the

first round of pellet collection. Regarding the phosphorylation status, there was again no considerable difference in the phosphorylation of 4E-BP1 in the lymphoma cell lines in comparison to the control B-cell line. However, there appeared to be increased phosphorylation of eIF2α in the lymphoma cell lines in this round of pellet collection, in contrast to the first one (**Figure 17B**).

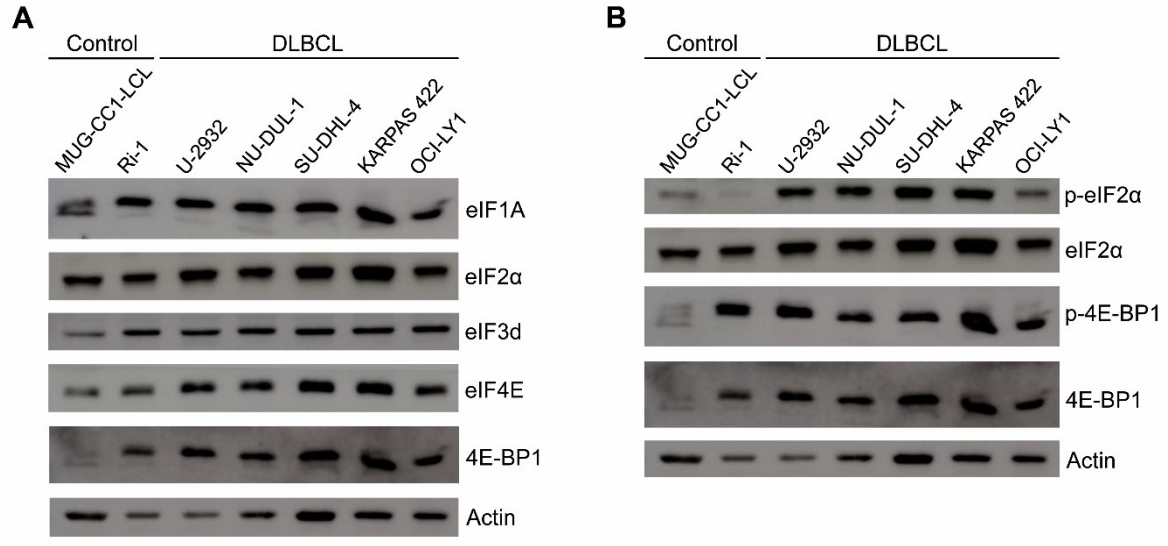

Figure 17: Western blot analysis of eIF expression (A) and phosphorylation (B) in DLBCL cell lines (DLBCL) and a control B-cell line (Control) – Repeated analysis. Actin was used as a loading control. Signals were detected and images were taken using the ImageQuant LAS 500. Abbreviations: phosho-eIF2α (p-eIF2α), phospho-4E-BP1 (p-4E-BP1).

To sum up the results, the cell line investigations could confirm the overexpression of eIF1A and eIF3d, but also that of eIF2α, eIF4E and 4E-BP1, in DLBCL by Western blot analysis on the protein level.

3.3 The mRNA expression pattern of *EIF2B5*, *EIF4E* and *EIF5* correlates with patient survival in the study cohort

To investigate possible links between eIF expression and patient outcome and to further analyze the role of eIFs in DLBCL pathogenesis, eIF mRNA expression in the study cohort was exploratively set in relation to patient survival. Importantly, 3 out of the 16 eIFs tested, namely *EIF2B5*, *EIF4E* and *EIF5*, indeed showed strong associations between their expression pattern and cancer-specific survival time. When dividing the patient cohort into two groups using the 3rd quartile of the respective eIF expression levels, the analysis revealed for all three eIFs that the group with higher eIF expression was associated with worse patient outcome (p=0.005 for *EIF2B5*, p=0.017 for *EIF4E*, p=0.001 for *EIF5*, **Figure 18**).

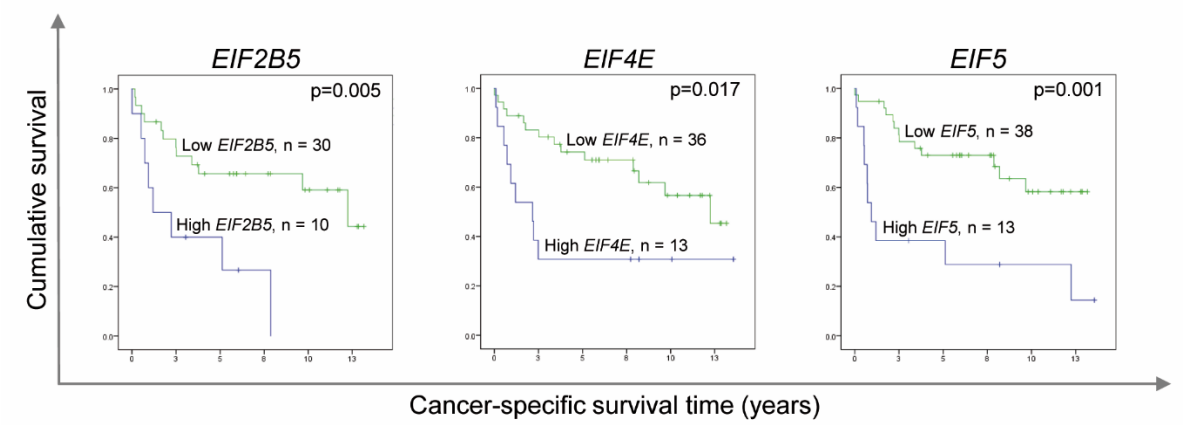

Figure 18: Analysis of patient outcome in relation to *EIF2B5*, *EIF4E* and *EIF5* mRNA expression in the study cohort. Green color indicates patients with lower eIF expression than the 3rd quartile of the respective mRNA levels of the study cohort, blue color indicates patients with higher eIF expression. Reproduced with modifications from (128). [http://creativecommons.org/licenses/by/4.0/]

3.4 Validation of the prognostic properties of *EIF2B5*/eIF2B5 expression using different approaches

3.4.1 Validation in two external patient cohorts

To validate the detected association between eIF expression and patient survival also in an independent cohort, two publicly available DLBCL patient cohorts were investigated. As external cohorts, the mRNA expression data sets published by Shipp *et al.* (132) (n=58) and Lenz *et al.* (47) (n=200) were used.

To compare the different cohorts, a summary of patient characteristics in the two external patient cohorts mentioned above and the study cohort is provided in **Table 7**. Comparison of clinicopathologic parameters showed that the Shipp and the Lenz cohort generally had lower IPI scores than those present in the study cohort. Further information on age, Ann Arbor Stage, and DLBCL subtype distribution was only available from the Lenz cohort. This information revealed that the patients of the Lenz cohort showed an Ann Arbor Stage and DLBCL subtype distribution similar to that of the study cohort, but were younger in general (see **Table 7**).

Table 7: Comparison between patient characteristics in the study cohort and in the publicly available Shipp (132) and Lenz (47) cohort. In the Shipp data set, only the IPI was reported, therefore all other parameters are not applicable (na) in this case. The percentage within the cohort was calculated by dividing the number of patients with the indicated parameter characteristic by the number of patients with information about this clinicopathologic parameter. Reproduced with modifications from (128). [http://creativecommons.org/licenses/by/4.0/]

Clinicopathologic parameter	Study cohort	Shipp cohort	Lenz cohort
Treatment regimen	R-CHOP-like regimen	CHOP-like combination chemotherapy	R-CHOP-like regimen
Total patient number	56	58	200
Age (years)			
>60	44/56 (79%)	na	109/200 (54%)
Ann Arbor Stage			
>II	34/55 (62%)	na	105/194 (54%)
DLBCL subtype			
GCB	34/53 (64%)	na	107/200 (54%)
nGCB/ABC	19/53 (36%)	na	93/200 (46%)
IPI (IPI score)			
Low (0-1)	15/54 (28%)	26/56 (46%)	62/156 (40%)
Intermediate (2-3)	27/54 (50%)	28/56 (50%)	73/156 (47%)
High (4-5)	12/54(22%)	2/56 (4%)	21/156 (13%)

Abbreviations: GCB-DLBCL (GCB), nGCB-DLBCL (nGCB), ABC-DLBCL (ABC); In the study cohort and Lenz cohort, the DLBCL subtype was determined in a different way, nevertheless both differently determined subtypes are shown in one row to ease comparison.

Importantly, it was the prognostic potential of *EIF2B5* that could be confirmed in both external patient cohorts. In the Shipp and Lenz cohort, high *EIF2B5* mRNA expression was also associated with worse patient survival (p=0.006 and p=0.014, respectively, **Figure 19**).

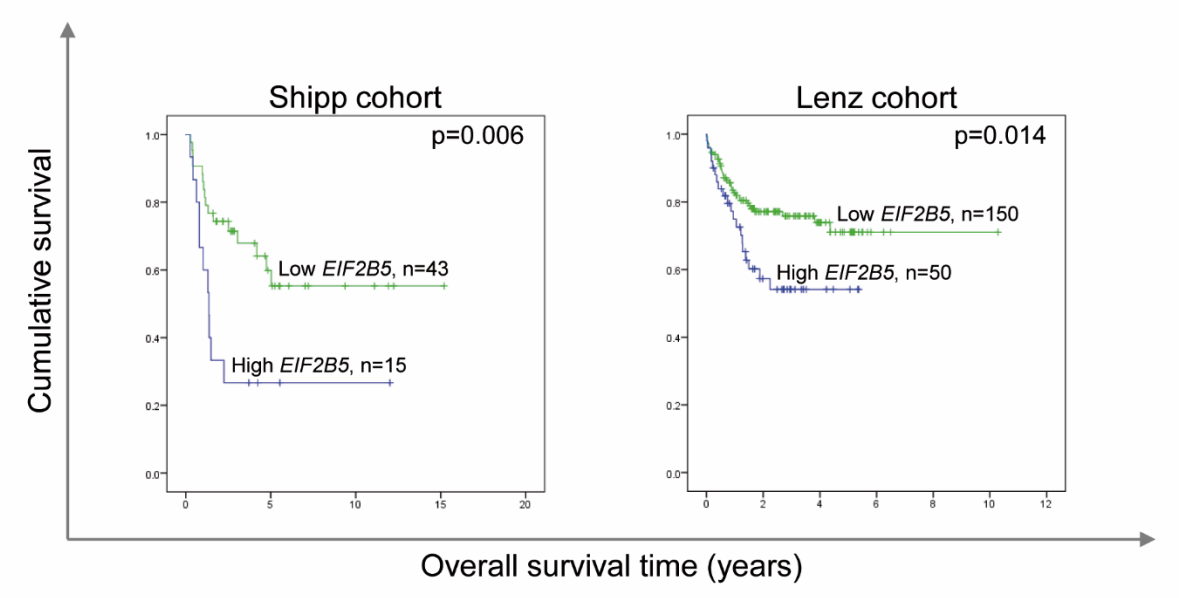

Figure 19: Analysis of patient outcome in relation to *EIF2B5* mRNA expression in the Shipp (132) and the Lenz (47) data set. Green color indicates patients with lower *EIF2B5* expression than the 3rd quartile of the respective mRNA levels of each cohort, blue color indicates patients with higher *EIF2B5* expression. Reproduced with modifications from (128). [http://creativecommons.org/licenses/by/4.0/]

3.4.2 Validation on the protein level

The survival analyses so far revealed that *EIF2B5* mRNA levels seemed to be associated with patient outcome. To investigate whether this is also true for eIF2B5 protein levels, the immunohistochemical stainings of the study cohort were used again. Patients with an immunohistochemical eIF2B5 staining intensity of score 3 were thereby opposed to the rest of the patient cohort regarding their outcome. This highest score 3 was seen in approximately one quarter of all study patients, and the division was thus comparable to that produced by the 3rd quartile in mRNA expression analysis.

Remarkably, this group of patients rated with score 3, indicating the highest eIF2B5 protein expression, again experienced worse outcome (**Figure 20**, p=0.006).

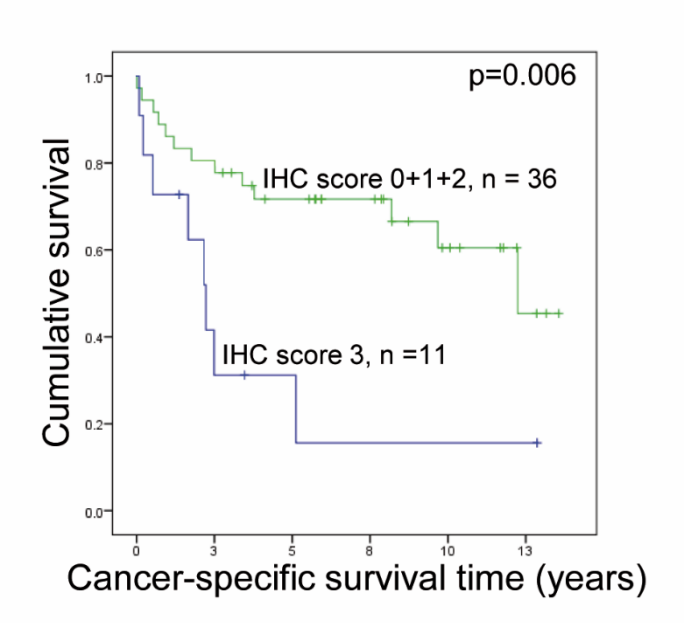

Figure 20: Analysis of patient outcome in relation to eIF2B5 protein expression in the study cohort determined by IHC. Reproduced with modifications from (128). [http://creativecommons.org/licenses/by/4.0/]

This result is in line with the prognostic potential of *EIF2B5* mRNA expression and confirms it on the protein level. Furthermore, IHC is a method used in routine pathology and would therefore enable analysis of eIF2B5 expression in daily diagnostic routine.

3.4.3 Validation by multivariate analysis

In the univariate setting, high *EIF2B5*/eIF2B5 expression was linked to worse patient survival in the study cohort as well as in two external patient cohorts. To investigate potential influencing factors in this regard, a multivariate analysis was performed with the mRNA data of the study cohort by using the Cox proportional hazards model, adjusting for the covariates “sex”, “age”, “DLBCL subtype” and “Ann Arbor Stage”. (**Table 8**).

First, in addition to the multivariate analysis, a univariate analysis using the Cox proportional hazards model was performed. In the univariate set-up, the covariates “age” ($p=0.011$), “DLBCL subtype” ($p<0.001$) and “*EIF2B5* expression” ($p=0.008$) were associated with patient outcome. This confirmed the results of the univariate

log-rank test regarding *EIF2B5* expression and patient survival in the study cohort (compare **Figure 18**).

In the multivariate set-up, advanced Ann Arbor Stage of the patients also became associated with worse outcome (p=0.006). Furthermore, presence of nGCB-DLBCL subtype (p=0.002) and, importantly, also high *EIF2B5* expression (p=0.003) remained linked to worse survival, as in the univariate analysis. Of note, the hazard ratio of "*EIF2B5* expression" increased from 3.562 in the univariate setting to 5.615 in the multivariate setting.

These results of the multivariate analysis of the study cohort thus revealed that high *EIF2B5* levels were associated with worse outcome independently from the other covariates tested, and thereby once more strengthened the prognostic potential of this eIF in DLBCL.

Table 8: Multivariate analysis of cancer-specific survival time in relation to *EIF2B5* mRNA expression levels in the study cohort. The multivariate analysis was performed using the Cox proportional hazards model. "Low" *EIF2B5* expression indicates patients with *EIF2B5* mRNA levels below the 3rd quartile of *EIF2B5* levels of the study cohort and "high" *EIF2B5* expression indicates those with *EIF2B5* mRNA levels above the 3rd quartile. "HR" denotes the hazard ratio of the second group in comparison to the first. The corresponding lower and upper 95% confidence interval is depicted as "Lo 95% CI" and "Up 95% CI", respectively. Reproduced with modifications from (128). [http://creativecommons.org/licenses/by/4.0/]

	1st group	2nd group	HR	Lo 95% CI	Up 95% CI	p-value
			Univariate			
Sex	female, n=27	male, n=27	1.674	0.732	3.832	0.222
Age	continuous		1.054	1.012	1.098	**0.011**
Ann Arbor Stage	I+II, n=20	III+IV, n=34	2.104	0.824	5.371	0.120
DLBCL subtype	GCB, n=32	nGCB, n=19	7.551	2.845	20.037	**<0.001**
EIF2B5 expression	low, n=30	high, n=10	3.562	1.390	9.131	**0.008**
			Multivariate			
Sex	female, n=18	male, n=19	1.624	0.536	4.917	0.391
Age	continuous		1.057	0.997	1.121	0.064
Ann Arbor Stage	I+II, n=11	III+IV, n=26	7.121	1.778	28.520	**0.006**
DLBCL subtype	GCB, n=23	nGCB, n=14	7.422	2.073	26.576	**0.002**
EIF2B5 expression	low, n=28	high, n=9	5.615	1.765	17.863	**0.003**

Abbreviations: GCB-DLBCL (GCB), nGCB-DLBCL (nGCB).

4 Discussion

Cell division is coupled with cell growth and thus also with protein synthesis, as proteins often represent the most plentiful macromolecules in proliferating cells. A key control point in the process of protein translation is its initiation, and experiments with yeast mutant strains have shown that translation initiation factors are directly connected with the ability of cells to start a new round of cell division (137). Importantly, one fundamental characteristic of cancer cells is the fact that they show chronic proliferation (138). When considering furthermore that lymphocytes, which get activated to proliferate, reveal even in the non-malignant setting an induction of eIF-expression that contributes to their increased protein synthesis (139), it seems to be a logical consequence that deregulation of eIFs has been demonstrated to be connected with a wide range of different cancer entities (57, 58) and that eIFs have in particular also been shown to be involved in lymphomagenesis and lymphoma biology (see e.g. (104, 105, 124)).

Nevertheless, analyzing the contribution of eIFs to malignancies and in particular to DLBCL, most studies focused on commonly investigated factors and therefore on commonly investigated parts of the translation initiation pathway (most often eIF4-factors) (63, 66, 81, 112, 115). In contrast, in the present study, 16 different eIFs, implicated in various parts of the translation initiation pathway, were tested for their mRNA expression profile in DLBCL. Importantly, this analysis revealed an overexpression of 12 out of these 16 eIFs tested in DLBCL, revealing dysregulation across all tested parts of the translation initiation pathway (“eIF2-cycle and eIF2A”, “eIF3-subunits”, “eIF1 and eIF1A” and “eIF4-factors”).

Many of the eIFs tested have never been investigated in DLBCL before. However, already existing data on a few factors allow for a comparison between the study results and the current literature. As such, eIF4E overexpression in DLBCL has already been reported (113), what confirms the results of this study. This is also in line with the reported disease involvement of eIF4E, reflected, e.g., by its contribution to the pathogenesis of DH/TH DLBCLs (127). Moreover, similar to the present investigation, higher expression of 4E-BP1 in DLBCL has also already been reported by two previous studies (115, 119). Finally, in the present expression analysis, *EIF4G3* (also referred to as *EIF4GII*) was one of the eIFs that

did not reveal considerably higher mRNA levels in DLBCL. However, interestingly, in a previous study, Mazan-Mamczarz *et al.* described, in contrast, overexpression of eIF4GII in DLBCL on the protein level (the mRNA level was not analyzed). In that study, the authors furthermore reported the eIF mRNA to be targeted by miR-520c-3p, a microRNA displaying an inverse expression pattern that is lower in DLBCL than in normal B-cells (118). Combined with our study results, this therefore indicates important expression regulation of eIF4GII by post-transcriptional mechanisms.

Besides overexpression of most eIFs tested in DLBCL, a further important observation of this study was the large number of eIFs (especially members of the "eIF2-cycle and eIF2A") showing higher expression in the nGCB-DLBCL subtype when compared to the GCB-DLBCL subtype. Using IHC analysis, Demosthenous *et al.* have already compared eIF4E expression in the GCB-DLBCL and ABC-DLBCL subtype. In contrast to the present study, they did not detect a subtype-specific expression pattern of eIF4E (112). However, this could be due to a different scoring system used (only positive and negative staining was distinguished), which could have been less sensitive than the one applied in the present study. It is known that the nGCB-DLBCL subtype is linked to worse patient outcome and thus to a more aggressive disease behavior (10). Importantly, Wang *et al.* have previously shown that the expression levels of eIF2α and eIF4E increase from less aggressive to highly aggressive lymphomas and thus correlate with lymphoma aggressiveness (104). This connection is also in line with results from other malignancies, where higher expression of eIFs has been linked to poorer tumor differentiation, higher incidence of metastasis and worse outcome (140, 141). Thus, the herein detected higher expression of eIFs in the nGCB-DLBCL subtype could be further proof for their association with a more aggressive neoplastic phenotype.

Considering the results of the above discussed explorative mRNA expression characterization in DLBCL and non-neoplastic germinal center B-cells, three eIFs arose special interest: eIF1A, eIF3d and eIF2B5. All three have never been linked to the pathogenesis of DLBCL before, but showed in the present analysis considerably strong overexpression in DLBCL.

eIF1A is involved in PIC assembly and in the process of start codon screening (58). Mutations of its gene have been shown to be associated with cancer (75, 76). Besides that, however, not that much is known about eIF1A in the neoplastic setting at present. Importantly, the present study reports eIF1A overexpression in DLBCL on the mRNA and protein level.

Together with 12 other subunits, eIF3d is a member of the eIF3-complex, which performs multiple tasks within translation initiation, including stabilization of the binding of the ternary complex to the small ribosomal subunit and also mRNA recruitment to it (58). Previous studies have already reported important roles of eIF3d in the pathogenesis of different cancer entities, ranging from gastric cancer to ovarian cancer or gallbladder cancer (98-100). Recently, eIF3d came in further focus of research, because it was identified as a novel cap-binding protein that enables a cap-dependent translation initiation mechanism independent of eIF4E. Through its cap-binding activity, eIF3d seems to direct the eIF3-complex and therefore the translational machinery to a specific set of mRNAs, leading to a specialized translational program particularly supporting cell proliferation (96, 97). Also, in the mRNA expression analysis of the present study, eIF3d stood out of the other eIF3-subunits tested, as it was the only one that showed marked overexpression in DLBCL. Confirmation on the protein level then furthermore strengthened its role in DLBCL pathogenesis. It is not clear which mechanism causes the higher expression of eIF3d in DLBCL, but considering the recent findings, its overexpression might support the aggressive phenotype of the disease by sustaining cell proliferation.

eIF2B5 holds the catalytic activity of eIF2B, which is necessary for eIF2 reactivation and thus for Met-tRNA$_i$ recruitment to the ribosome during translation initiation (78, 79). Besides its role in regular cell metabolism, eIF2B5 has, however, also been described in the pathological setting. *EIF2B5* gene mutations have been linked to an inherited disorder referred to as leukoencephalopathy with vanishing white matter (83). Moreover, eIF2B5 has been also reported to be overexpressed in different cancer entities (84, 85). Nevertheless, this study is the first to assign eIF2B5 a particular role in DLBCL pathogenesis, by revealing its overexpression in DLBCL and its higher expression in the nGCB-DLBCL subtype on the mRNA and protein level. Importantly, *EIF2B5* is located on chromosome 3

(3q27) (142). Therefore, one could speculate that its overexpression might be potentially linked to the frequent gains of chromosome 3 observed in DLBCL and especially in the ABC-DLBCL subtype. 26% of ABC-DLBCLs show gains of the whole 3q-arm, 15% even trisomy 3 (45). This would also be in line with its higher expression in the nGCB-DLBCL subtype. However, this cannot explain the also considerable overexpression of the other two eIF2B-members analyzed in this study and located on different chromosomes (142). Moreover, *EIF2A* is also located on chromosome 3 (143), but in the present analysis, *EIF2A* was not among those eIFs with considerably higher expression in DLBCL. Still, it could be possible that the chromosomal location of its gene is somehow implicated in the overexpression of eIF2B5 in DLBCL (and maybe also in the extraordinary role eIF2B5 took considering the whole study), although this would certainly need further examination. Namely, apart from its remarkable expression profile, the most important finding regarding eIF2B5 concerns its correlation with patient outcome, detected in the survival analysis and discussed in the following.

When analyzing patient survival in the context of eIF mRNA expression levels in the study cohort, an association between high *EIF2B5*, *EIF4E* and *EIF5* expression and worse patient outcome was detected. This result is in line with a previous IHC analysis of eIF4E, performed by Demosthenous *et al.* (112). Furthermore, in DLBCL, a similar relationship between high expression and worse patient outcome has already been demonstrated for eIF4B (not analyzed in the present study) (119), and also when reviewing the literature for other neoplastic entities, high eIF expression has frequently been associated with worse patient outcome (60, 61, 99).

However, one important limitation of the study cohort lies in its rather small patient number, especially when analyzing patient survival. Thus, the survival data were tested for confirmation in two publicly available DLBCL patient data sets. The Shipp data set (132) included a comparable number of patients (n=58), the Lenz data set (47), however, allowed for an analysis in a larger patient cohort (n=200). Importantly, the prognostic potential of *EIF2B5* mRNA expression could be confirmed in both external patient cohorts. Jiao *et al.* recently reported an association between high *EIF2B5* mRNA expression and worse patient outcome in liver cancer (85). Moreover, rare alleles of *EIF2B5* have been associated with

better prognosis in ovarian cancer (87). The results of the present study now propose a prognostic potential of *EIF2B5* in DLBCL.

An important drawback of expression analyses on the mRNA level is their limited clinical utility. One example represents the DLBCL subtype classification, which has been first presented using mRNA expression analyses, but later had to be translated into immunohistochemical algorithms, since microarray analysis is currently impractical for daily diagnostic routine (9, 11). Therefore, it is particularly noteworthy that also in the IHC analysis performed by using DLBCL specimens of the study cohort, strong eIF2B5 expression was again linked to worse patient outcome, confirming the mRNA data. This and its independence from other potential influencing factors, as revealed by multivariate analysis, strongly suggest possible usefulness of eIF2B5 as a novel prognostic marker in DLBCL used in daily clinical practice.

It is currently largely unknown, what mechanisms exactly cause overexpression of eIFs in cancer. Importantly, for some eIFs it has been reported that MYC enhances their transcription (110, 144). Nevertheless, this probably cannot explain the strongly deregulated mRNA expression profile of so many eIFs in DLBCL detected in the present study. Post-transcriptional mechanisms regulating eIF expression have also been investigated, as for example the above mentioned regulation of eIF4GII by miR-520c-3p.(118) For some eIFs, it has been shown that the mTOR signaling pathway might be post-transcriptionally implicated in their increased translation. Remarkably, this interplay with the mTOR signaling pathway has been reported in DLBCL cell lines for eIF4B (119) and especially also for eIF2B5 in rat fibroblasts (145).

The mTOR signaling pathway is known to play an important role in DLBCL. Amongst others, its activity can be determined by analyzing the phosphorylation status of 4E-BP1 (146). Nevertheless, in the present Western blot analysis, there was no considerable difference in 4E-BP1 phosphorylation detectable between control B-cell line and DLBCL cell lines, indicating similar mTOR activity. This result is in contrast to a previously performed study by Horvilleur *et al.*, who detected increased phosphorylation of 4E-BP1 in DLBCL cell lines (119). However, on the other hand, the result of the present study is in line with an IHC

study by Kodali *et al.* (115). In the present study, also the phosphorylation status of eIF2α was analyzed in the control B-cell line in comparison with the DLBCL cell lines and revealed a heterogeneous picture. Phosphorylation of eIF2α and thereby inhibition of eIF2-GDP recycling occurs during the integrated stress response (57). Increased phosphorylation of eIF2α and thus increased UPR activation has been reported for Burkitt's lymphoma and has been suggested to support the pathogenic role of MYC in this disease (106). In the present study, higher eIF2α phosphorylation was detected in one of two analyses performed and therefore did not yield a clear result, but a trend for a possibly higher UPR activation in DLBCL. In general, the analysis of the phosphorylation status of 4E-BP1 and eIF2α was complicated by the concomitant overexpression of the respective unphosphorylated protein in DLBCL and would thus need further in-depth analysis by using also a higher number of control B-cell lines and/or patient samples.

To conclude, the present study on the eIF expression profile in DLBCL revealed a strongly dysregulated translation initiation pathway that could be implicated in the pathogenesis of DLBCL. Nevertheless, the mechanisms causing the deregulation of this large number of different eIFs still remain to be elucidated. Furthermore, the investigation of functional consequences of a dysregulated translation initiation pathway in DLBCL development and progression could be a promising task for future studies. Possible methods for functional analyses could include the overexpression or downregulation of eIFs in DLBCL cell lines and the analysis of its effects. Of note, siRNA-mediated silencing of eIFs in DLBCL cell lines was performed in the present study (data not shown), but could not lead to a sufficient downregulation of eIF-expression measured by Western blot analysis of cell culture pellets. Difficulties in knockdown of eIFs in DLBCL cell lines have also been described in the literature: Virus-mediated knockdown of eIF4B and eIF4E was reported to be lethal for some DLBCL cell lines (120, 121). Thus, it might be possible that also in the present study, cells with successful downregulation of eIFs died and were overgrown by those with unsuccessful siRNA-mediated knockdown, what consequently prevented all further functional analyses. Therefore, overexpression of eIFs in DLBCL cell lines could be probably a more applicable tool for investigating the function of eIFs in DLBCL pathogenesis. Furthermore, the results of the present study suggest of course also the

investigation of eIF-inhibitors for DLBCL treatment. Inhibitors of eIF4-factors have already revealed great potential in studies using mouse lymphoma models and have partly also been tested in DLBCL (122-124, 126, 127). However, for eIF1A, eIF2B5 or eIF3d, so far no inhibitor exists, although the data presented herein would suggest an especially promising efficacy of eIF2B5 inhibition in DLBCL.

Apart from the uncovered strongly dysregulated translation initiation pathway in DLBCL, the most important finding of the present study might, however, be the potential of eIF2B5 to serve as a novel prognostic marker in DLBCL. Nevertheless, to find out whether eIF2B5 expression could be indeed used to stratify the patients' risk in daily clinical practice, it is necessary to analyze eIF2B5 in a larger patient cohort as a next step. Moreover, its efficacy must be also compared with that of already established prognostic markers, especially with the IPI. Thereby, one could further assess the prognostic potential of eIF2B5 in DLBCL and investigate whether the current promising data find also confirmation in different experimental set-ups.

5 Bibliography

1. Freedman J. Lymphoma: Current and Emerging Trends in Detection and Treatment. 1st ed. New York: The Rosen Publishing Group, Inc.; 2005.
2. STATISTIK AUSTRIA. Hodgkin (C81) - Krebsinzidenz (Neuerkrankungen pro Jahr), Österreich ab 1983 [Internet]. [cited 15th November 2018]. Available from: https://www.statistik.at/web_de/statistiken/menschen_und_gesellschaft/gesundheit/krebserkrankungen/hodgkin/021746.html.
3. STATISTIK AUSTRIA. Non-Hodgkin (C82-C86,C96) - Krebsinzidenz (Neuerkrankungen pro Jahr), Österreich ab 1983 [Internet]. [cited 15th November 2018]. Available from: https://www.statistik.at/web_de/statistiken/menschen_und_gesellschaft/gesundheit/krebserkrankungen/non-hodgkin/021786.html.
4. STATISTIK AUSTRIA. Myelom (C90) - Krebsinzidenz (Neuerkrankungen pro Jahr), Österreich ab 1983 [Internet]. [cited 15th November 2018]. Available from: https://www.statistik.at/web_de/statistiken/menschen_und_gesellschaft/gesundheit/krebserkrankungen/plasmozytom_myelom/107469.html.
5. Shanbhag S, Ambinder RF. Hodgkin lymphoma: A review and update on recent progress. CA Cancer J Clin. 2018;68:116-32.
6. Armitage JO, Gascoyne RD, Lunning MA, Cavalli F. Non-Hodgkin lymphoma. Lancet. 2017;390:298-310.
7. Martelli M, Ferreri AJM, Agostinelli C, Di Rocco A, Pfreundschuh M, Pileri SA. Diffuse large B-cell lymphoma. Crit Rev Oncol Hematol. 2013;87:146-71.
8. Pasqualucci L, Dalla-Favera R. The Genetic Landscape of Diffuse Large B-Cell Lymphoma. Semin Hematol. 2015;52:67-76.
9. Alizadeh AA, Eisen MB, Davis RE, Ma C, Lossos IS, Rosenwald A et al. Distinct types of diffuse large B-cell lymphoma identified by gene expression profiling. Nature. 2000;403:503-11.
10. Hans CP, Weisenburger DD, Greiner TC, Gascoyne RD, Delabie J, Ott G et al. Confirmation of the molecular classification of diffuse large B-cell lymphoma by immunohistochemistry using a tissue microarray. Blood. 2004;103:275-82.

11. Meyer PN, Fu K, Greiner TC, Smith LM, Delabie J, Gascoyne RD et al. Immunohistochemical Methods for Predicting Cell of Origin and Survival in Patients With Diffuse Large B-Cell Lymphoma Treated With Rituximab. J Clin Oncol. 2011;29:200-7.
12. Staudt LM, Dave S. The Biology of Human Lymphoid Malignancies Revealed by Gene Expression Profiling. In: Alt F, editor. Advances in Immunology. Vol 87. Cambridge: Academic Press; 2005. p. 163-208.
13. Schmitz R, Wright GW, Huang DW, Johnson CA, Phelan JD, Wang JQ et al. Genetics and Pathogenesis of Diffuse Large B-Cell Lymphoma. N Engl J Med. 2018;378:1396-407.
14. Riedell PA, Smith SM. Double hit and double expressors in lymphoma: Definition and treatment. Cancer. 2018.
15. Basso K, Dalla-Favera R. Germinal centres and B cell lymphomagenesis. Nat Rev Immunol. 2015;15:172-84.
16. Warrington R, Watson W, Kim HL, Antonetti FR. An introduction to immunology and immunopathology. Allergy Asthma Clin Immunol. 2011;7 Suppl 1:S1.
17. Golovkina TV, Shlomchik M, Hannum L, Chervonsky A. Organogenic Role of B Lymphocytes in Mucosal Immunity. Science. 1999;286:1965-8.
18. Nolte MA, Arens R, Kraus M, van Oers MHJ, Kraal G, van Lier RAW et al. B Cells Are Crucial for Both Development and Maintenance of the Splenic Marginal Zone. J Immunol. 2004;172:3620-7.
19. Iwata Y, Yoshizaki A, Komura K, Shimizu K, Ogawa F, Hara T et al. CD19, a Response Regulator of B Lymphocytes, Regulates Wound Healing through Hyaluronan-Induced TLR4 Signaling. Am J Pathol. 2009;175:649-60.
20. Harris DP, Haynes L, Sayles PC, Duso DK, Eaton SM, Lepak NM et al. Reciprocal regulation of polarized cytokine production by effector B and T cells. Nat Immunol. 2000;1:475-82.
21. Crawford A, MacLeod M, Schumacher T, Corlett L, Gray D. Primary T Cell Expansion and Differentiation In Vivo Requires Antigen Presentation by B Cells. J Immunol. 2006;176:3498-506.
22. Kuppers R. Mechanisms of B-cell lymphoma pathogenesis. Nat Rev Cancer. 2005;5:251-62.

23. Hwang JK, Alt FW, Yeap LS. Related Mechanisms of Antibody Somatic Hypermutation and Class Switch Recombination. Microbiol Spectr. 2015;3:Mdna3-0037-2014.
24. Hoehn KB, Fowler A, Lunter G, Pybus OG. The Diversity and Molecular Evolution of B-Cell Receptors during Infection. Mol Biol Evol. 2016;33:1147-57.
25. Abbas AK, Lichtman AH, Pillai S. Basic Immunology - Functions and Disorders of the Immune System. 4th ed. Philadelphia: Saunders; 2012.
26. Küppers R, Klein U, Hansmann M-L, Rajewsky K. Cellular Origin of Human B-Cell Lymphomas. N Engl J Med. 1999;341:1520-9.
27. Testoni M, Zucca E, Young KH, Bertoni F. Genetic lesions in diffuse large B-cell lymphomas. Ann Oncol. 2015;26:1069-80.
28. Pasqualucci L, Dominguez-Sola D, Chiarenza A, Fabbri G, Grunn A, Trifonov V et al. Inactivating mutations of acetyltransferase genes in B-cell lymphoma. Nature. 2011;471:189-95.
29. Iqbal J, Greiner TC, Patel K, Dave BJ, Smith L, Ji J et al. Distinctive patterns of BCL6 molecular alterations and their functional consequences in different subgroups of diffuse large B-cell lymphoma. Leukemia. 2007;21:2332-43.
30. Basso K, Dalla-Favera R. Roles of BCL6 in normal and transformed germinal center B cells. Immunol Rev. 2012;247:172-83.
31. Challa-Malladi M, Lieu YK, Califano O, Holmes AB, Bhagat G, Murty VV et al. Combined Genetic Inactivation of β2-Microglobulin and CD58 Reveals Frequent Escape from Immune Recognition in Diffuse Large B Cell Lymphoma. Cancer Cell. 2011;20:728-40.
32. Dominguez-Sola D, Kung J, Holmes AB, Wells VA, Mo T, Basso K et al. The FOXO1 Transcription Factor Instructs the Germinal Center Dark Zone Program. Immunity. 2015;43:1064-74.
33. Trinh DL, Scott DW, Morin RD, Mendez-Lago M, An J, Jones SJM et al. Analysis of FOXO1 mutations in diffuse large B-cell lymphoma. Blood. 2013;121:3666-74.
34. Pasqualucci L, Dalla-Favera R. Genetics of diffuse large B-cell lymphoma. Blood. 2018;131:2307-19.

35. Morin RD, Johnson NA, Severson TM, Mungall AJ, An J, Goya R et al. Somatic mutations altering EZH2 (Tyr641) in follicular and diffuse large B-cell lymphomas of germinal-center origin. Nat Genet. 2010;42:181-5.

36. Béguelin W, Popovic R, Teater M, Jiang Y, Bunting KL, Rosen M et al. EZH2 Is Required for Germinal Center Formation and Somatic EZH2 Mutations Promote Lymphoid Transformation. Cancer Cell. 2013;23:677-92.

37. Muppidi JR, Schmitz R, Green JA, Xiao W, Larsen AB, Braun SE et al. Loss of signalling via Gα13 in germinal centre B-cell-derived lymphoma. Nature. 2014;516:254-8.

38. Davis RE, Brown KD, Siebenlist U, Staudt LM. Constitutive Nuclear Factor κB Activity Is Required for Survival of Activated B Cell–like Diffuse Large B Cell Lymphoma Cells. J Exp Med. 2001;194:1861-74.

39. Davis RE, Ngo VN, Lenz G, Tolar P, Young RM, Romesser PB et al. Chronic active B-cell-receptor signalling in diffuse large B-cell lymphoma. Nature. 2010;463:88-92.

40. Lenz G, Davis RE, Ngo VN, Lam L, George TC, Wright GW et al. Oncogenic CARD11 Mutations in Human Diffuse Large B Cell Lymphoma. Science. 2008;319:1676-9.

41. Compagno M, Lim WK, Grunn A, Nandula SV, Brahmachary M, Shen Q et al. Mutations of multiple genes cause deregulation of NF-κB in diffuse large B-cell lymphoma. Nature. 2009;459:717-21.

42. Ngo VN, Young RM, Schmitz R, Jhavar S, Xiao W, Lim K-H et al. Oncogenically active MYD88 mutations in human lymphoma. Nature. 2010;470:115-9.

43. Pasqualucci L, Compagno M, Houldsworth J, Monti S, Grunn A, Nandula SV et al. Inactivation of the PRDM1/BLIMP1 gene in diffuse large B cell lymphoma. J Exp Med. 2006;203:311-7.

44. Calado DP, Zhang B, Srinivasan L, Sasaki Y, Seagal J, Unitt C et al. Constitutive Canonical NF-kB Activation Cooperates with Disruption of BLIMP1 in the Pathogenesis of Activated B Cell-like Diffuse Large Cell Lymphoma. Cancer Cell. 2010;18:580-9.

45. Bea S, Zettl A, Wright G, Salaverria I, Jehn P, Moreno V et al. Diffuse large B-cell lymphoma subgroups have distinct genetic profiles that influence tumor biology and improve gene-expression-based survival prediction. Blood. 2005;106:3183-90.
46. Scott DW, Gascoyne RD. The tumour microenvironment in B cell lymphomas. Nat Rev Cancer. 2014;14:517-34.
47. Lenz G, Wright G, Dave SS, Xiao W, Powell J, Zhao H et al. Stromal gene signatures in large-B-cell lymphomas. N Engl J Med. 2008;359:2313-23.
48. Sehn LH, Gascoyne RD. Diffuse large B-cell lymphoma: optimizing outcome in the context of clinical and biologic heterogeneity. Blood. 2015;125:22-32.
49. Younes A, Ansell S, Fowler N, Wilson W, de Vos S, Seymour J et al. The landscape of new drugs in lymphoma. Nat Rev Clin Oncol. 2016;14:335-46.
50. Vaidya R, Witzig TE. Prognostic factors for diffuse large B-cell lymphoma in the R(X)CHOP era. Ann Oncol. 2014;25:2124-33.
51. Project TIN-HsLPF. A Predictive Model for Aggressive Non-Hodgkin's Lymphoma. N Engl J Med. 1993;329:987-94.
52. Sonenberg N, Hinnebusch AG. Regulation of Translation Initiation in Eukaryotes: Mechanisms and Biological Targets. Cell. 2009;136:731-45.
53. Steitz TA. A structural understanding of the dynamic ribosome machine. Nat Rev Mol Cell Biol. 2008;9:242-53.
54. Aitken CE, Lorsch JR. A mechanistic overview of translation initiation in eukaryotes. Nat Struct Mol Biol. 2012;19:568-76.
55. Shatsky IN, Terenin IM, Smirnova VV, Andreev DE. Cap-Independent Translation: What's in a Name? Trends Biochem Sci. 2018;43:882-95.
56. Sonenberg N, Hinnebusch AG. New Modes of Translational Control in Development, Behavior, and Disease. Mol Cell. 2007;28:721-9.
57. Chu J, Cargnello M, Topisirovic I, Pelletier J. Translation Initiation Factors: Reprogramming Protein Synthesis in Cancer. Trends Cell Biol. 2016;26:918-33.
58. Spilka R, Ernst C, Mehta AK, Haybaeck J. Eukaryotic translation initiation factors in cancer development and progression. Cancer Lett. 2013;340:9-21.
59. Lazaris-Karatzas A, Montine KS, Sonenberg N. Malignant transformation by a eukaryotic initiation factor subunit that binds to mRNA 5' cap. Nature. 1990;345:544-7.

60. De Benedetti A, Graff JR. eIF-4E expression and its role in malignancies and metastases. Oncogene. 2004;23:3189-99.

61. Cha Y-L, Li P-D, Yuan L-J, Zhang M-Y, Zhang Y-J, Rao H-L et al. EIF4EBP1 Overexpression Is Associated with Poor Survival and Disease Progression in Patients with Hepatocellular Carcinoma. PLoS One. 2015;10:e0117493.

62. Rojo F, Najera L, Lirola J, Jiménez J, Guzmán M, Sabadell MD et al. 4E-Binding Protein 1, A Cell Signaling Hallmark in Breast Cancer that Correlates with Pathologic Grade and Prognosis. Clin Cancer Res. 2007;13:81-9.

63. Zhang T, Guo J, Li H, Wang J. Meta-analysis of the prognostic value of p-4EBP1 in human malignancies. Oncotarget. 2018;9:2761-9.

64. Fukuchi-Shimogori T, Ishii I, Kashiwagi K, Mashiba H, Ekimoto H, Igarashi K. Malignant Transformation by Overproduction of Translation Initiation Factor eIF4G. Cancer Res. 1997;57:5041-4.

65. Silvera D, Arju R, Darvishian F, Levine PH, Zolfaghari L, Goldberg J et al. Essential role for eIF4GI overexpression in the pathogenesis of inflammatory breast cancer. Nat Cell Biol. 2009;11:903-8.

66. Eberle J, Krasagakis K, Orfanos CE. Translation initiation factor eIF-4A1 mRNA is consistently overexpressed in human melanoma cells in vitro. Int J Cancer. 1997;71:396-401.

67. Modelska A, Turro E, Russell R, Beaton J, Sbarrato T, Spriggs K et al. The malignant phenotype in breast cancer is driven by eIF4A1-mediated changes in the translational landscape. Cell Death Dis. 2015;6:e1603.

68. Shaoyan X, Juanjuan Y, Yalan T, Ping H, Jianzhong L, Qinian W. Downregulation of EIF4A2 in Non-Small-Cell Lung Cancer Associates with Poor Prognosis. Clin Lung Cancer. 2013;14:658-65.

69. Yang J, Wang J, Chen K, Guo G, Xi R, Rothman PB et al. eIF4B Phosphorylation by Pim Kinases Plays a Critical Role in Cellular Transformation by Abl Oncogenes. Cancer Res. 2013;73:4898-908.

70. Vaysse C, Philippe C, Martineau Y, Quelen C, Hieblot C, Renaud C et al. Key contribution of eIF4H-mediated translational control in tumor promotion. Oncotarget. 2015;6:39924-40.

71. Sheikh MS, Fornace Jr AJ. Regulation of translation initiation following stress. Oncogene. 1999;18:6121-8.

72. Lian Z, Pan J, Liu J, Zhang S, Zhu M, Arbuthnot P et al. The translation initiation factor, hu-Sui1 may be a target of hepatitis B X antigen in hepatocarcinogenesis. Oncogene. 1999;18:1677-87.

73. Golob-Schwarzl N, Schweiger C, Koller C, Krassnig S, Gogg-Kamerer M, Gantenbein N et al. Separation of low and high grade colon and rectum carcinoma by eukaryotic translation initiation factors 1, 5 and 6. Oncotarget. 2017;8:101224-43.

74. Yi T, Arthanari H, Akabayov B, Song H, Papadopoulos E, Qi HH et al. eIF1A augments Ago2-mediated Dicer-independent miRNA biogenesis and RNA interference. Nat Commun. 2015;6:7194.

75. Martin M, Masshofer L, Temming P, Rahmann S, Metz C, Bornfeld N et al. Exome sequencing identifies recurrent somatic mutations in EIF1AX and SF3B1 in uveal melanoma with disomy 3. Nat Genet. 2013;45:933-6.

76. Karunamurthy A, Panebianco F, Hsiao SJ, Vorhauer J, Nikiforova MN, Chiosea S et al. Prevalence and phenotypic correlations of EIF1AX mutations in thyroid nodules. Endocr Relat Cancer. 2016;23:295-301.

77. Martin-Marcos P, Zhou F, Karunasiri C, Zhang F, Dong J, Nanda J et al. eIF1A residues implicated in cancer stabilize translation preinitiation complexes and favor suboptimal initiation sites in yeast. Elife. 2017;6:e31250.

78. Jennings MD, Pavitt GD. eIF5 is a dual function GAP and GDI for eukaryotic translational control. Small GTPases. 2010;1:118-23.

79. Tsai JC, Miller-Vedam LE, Anand AA, Jaishankar P, Nguyen HC, Renslo AR et al. Structure of the nucleotide exchange factor eIF2B reveals mechanism of memory-enhancing molecule. Science. 2018;359:eaaq0939.

80. Rosenwald IB, Wang S, Savas L, Woda B, Pullman J. Expression of translation initiation factor eIF-2α is increased in benign and malignant melanocytic and colonic epithelial neoplasms. Cancer. 2003;98:1080-8.

81. Rosenwald IB, Hutzler MJ, Wang S, Savas L, Fraire AE. Expression of eukaryotic translation initiation factors 4E and 2α is increased frequently in bronchioloalveolar but not in squamous cell carcinomas of the lung. Cancer. 2001;92:2164-71.

82. Tanaka I, Sato M, Kato T, Goto D, Kakumu T, Miyazawa A et al. eIF2β, a subunit of translation-initiation factor EIF2, is a potential therapeutic target for non-small cell lung cancer. Cancer Sci. 2018;109:1843-52.
83. Bugiani M, Boor I, Powers JM, Scheper GC, van der Knaap MS. Leukoencephalopathy With Vanishing White Matter: A Review. J Neuropathol Exp Neurol. 2010;69:987-96.
84. Balachandran S, Barber GN. Defective translational control facilitates vesicular stomatitis virus oncolysis. Cancer Cell. 2004;5:51-65.
85. Jiao Y, Fu Z, Li Y, Meng L, Liu Y. High EIF2B5 mRNA expression and its prognostic significance in liver cancer: a study based on the TCGA and GEO database. Cancer Manag Res. 2018;10:6003-14.
86. Gallagher JW, Kubica N, Kimball SR, Jefferson LS. Reduced Eukaryotic Initiation Factor 2Bε-Subunit Expression Suppresses the Transformed Phenotype of Cells Overexpressing the Protein. Cancer Res. 2008;68:8752-60.
87. Goode EL, Maurer MJ, Sellers TA, Phelan CM, Kalli KR, Fridley BL et al. Inherited Determinants of Ovarian Cancer Survival. Clin Cancer Res. 2010;16:995-1007.
88. Palaniappan A, Ramar K, Ramalingam S. Computational Identification of Novel Stage-Specific Biomarkers in Colorectal Cancer Progression. PLoS One. 2016;11:e0156665.
89. Brady LK, Wang H, Radens CM, Bi Y, Radovich M, Maity A et al. Transcriptome analysis of hypoxic cancer cells uncovers intron retention in EIF2B5 as a mechanism to inhibit translation. PLoS Biol. 2017;15:e2002623.
90. Rothe M, Ko Y, Albers P, Wernert N. Eukaryotic Initiation Factor 3 p110 mRNA Is Overexpressed in Testicular Seminomas. Am J Pathol. 2000;157:1597-604.
91. Shen J, Yin J-Y, Li X-P, Liu Z-Q, Wang Y, Chen J et al. The Prognostic Value of Altered eIF3a and Its Association with p27 in Non-Small Cell Lung Cancers. PLoS One. 2014;9:e96008.
92. Spilka R, Ernst C, Bergler H, Rainer J, Flechsig S, Vogetseder A et al. eIF3a is over-expressed in urinary bladder cancer and influences its phenotype independent of translation initiation. Cell Oncol (Dordr). 2014;37:253-67.

93. Nupponen NN, Porkka K, Kakkola L, Tanner M, Persson K, Borg Å et al. Amplification and Overexpression of p40 Subunit of Eukaryotic Translation Initiation Factor 3 in Breast and Prostate Cancer. Am J Pathol. 1999;154:1777-83.
94. Doldan A, Chandramouli A, Shanas R, Bhattacharyya A, Cunningham JT, Nelson MA et al. Loss of the Eukaryotic Initiation Factor 3f in Pancreatic Cancer. Mol Carcinog. 2008;47:235-44.
95. Scoles DR, Yong WH, Qin Y, Wawrowsky K, Pulst SM. Schwannomin inhibits tumorigenesis through direct interaction with the eukaryotic initiation factor subunit c (eIF3c). Hum Mol Genet. 2006;15:1059-70.
96. Lee ASY, Kranzusch PJ, Cate JHD. eIF3 targets cell-proliferation messenger RNAs for translational activation or repression. Nature. 2015;522:111-4.
97. Lee ASY, Kranzusch PJ, Doudna JA, Cate JHD. eIF3d is an mRNA cap-binding protein that is required for specialized translation initiation. Nature. 2016;536:96-9.
98. Lin Y, Zhang R, Zhang P. Eukaryotic translation initiation factor 3 subunit D overexpression is associated with the occurrence and development of ovarian cancer. FEBS Open Bio. 2016;6:1201-10.
99. He J, Wang X, Cai J, Wang W, Qin X. High expression of eIF3d is associated with poor prognosis in patients with gastric cancer. Cancer Manag Res. 2017;9:539-44.
100. Zhang F, Xiang S, Cao Y, Li M, Ma Q, Liang H et al. EIF3D promotes gallbladder cancer development by stabilizing GRK2 kinase and activating PI3K-AKT signaling pathway. Cell Death Dis. 2017;8:e2868.
101. Hershey JWB. The role of eIF3 and its individual subunits in cancer. Biochim Biophys Acta Gene Regul Mech. 2015;1849:792-800.
102. Zhou M, Sandercock AM, Fraser CS, Ridlova G, Stephens E, Schenauer MR et al. Mass spectrometry reveals modularity and a complete subunit interaction map of the eukaryotic translation factor eIF3. Proc Natl Acad Sci U S A. 2008;105:18139-44.
103. Wagner S, Herrmannová A, Malík R, Peclinovská L, Valášek LS. Functional and Biochemical Characterization of Human Eukaryotic Translation Initiation Factor 3 in Living Cells. Mol Cell Biol. 2014;34:3041-52.

104. Wang S, Rosenwald IB, Hutzler MJ, Pihan GA, Savas L, Chen JJ et al. Expression of the Eukaryotic Translation Initiation Factors 4E and 2alpha in Non-Hodgkin's Lymphomas. Am J Pathol. 1999;155:247-55.
105. Ruggero D, Montanaro L, Ma L, Xu W, Londei P, Cordon-Cardo C et al. The translation factor eIF-4E promotes tumor formation and cooperates with c-Myc in lymphomagenesis. Nat Med. 2004;10:484-6.
106. Hart LS, Cunningham JT, Datta T, Dey S, Tameire F, Lehman SL et al. ER stress–mediated autophagy promotes Myc-dependent transformation and tumor growth. J Clin Invest. 2012;122:4621-34.
107. Wendel H-G, Stanchina Ed, Fridman JS, Malina A, Ray S, Kogan S et al. Survival signalling by Akt and eIF4E in oncogenesis and cancer therapy. Nature. 2004;428:332-7.
108. Wendel H-G, Silva RLA, Malina A, Mills JR, Zhu H, Ueda T et al. Dissecting eIF4E action in tumorigenesis. Genes Dev. 2007;21:3232-7.
109. Lin C-J, Nasr Z, Premsrirut PK, Porco JA, Jr., Hippo Y, Lowe SW et al. Targeting Synthetic Lethal Interactions between Myc and the eIF4F Complex Impedes Tumorigenesis. Cell Rep. 2012;1:325-33.
110. Lin C-J, Cencic R, Mills JR, Robert F, Pelletier J. c-Myc and eIF4F Are Components of a Feedforward Loop that Links Transcription and Translation. Cancer Res. 2008;68:5326-34.
111. Miluzio A, Beugnet A, Grosso S, Brina D, Mancino M, Campaner S et al. Impairment of Cytoplasmic eIF6 Activity Restricts Lymphomagenesis and Tumor Progression without Affecting Normal Growth. Cancer Cell. 2011;19:765-75.
112. Demosthenous C, Han JJ, Stenson MJ, Maurer MJ, Wellik LE, Link B et al. Translation initiation complex eIF4F is a therapeutic target for dual mTOR kinase inhibitors in non-Hodgkin lymphoma. Oncotarget. 2015;6:9488-501.
113. Culjkovic B, Fernando T, Yang S, Melnick AM, Borden KLB, Cerchietti L. The Eukaryotic Translation Initiation Factor 4E (eIF4E) Has Oncogenic Functions and May Represent a New Therapeutic Target In Diffuse Large B Cell Lymphoma (DLBCL). Blood. 2013;122:3785.
114. Landon AL, Muniandy PA, Shetty AC, Lehrmann E, Volpon L, Houng S et al. MNKs act as a regulatory switch for eIF4E1 and eIF4E3 driven mRNA translation in DLBCL. Nat Commun. 2014;5:5413.

115. Kodali D, Rawal A, Ninan MJ, Patel MR, Mesa H, Knapp D et al. Expression and Phosphorylation of Eukaryotic Translation Initiation Factor 4E Binding Protein 1 in B-Cell Lymphomas and Reactive Lymphoid Tissues. Arch Pathol Lab Med. 2011;135:365-71.
116. Ninan MJ, Rawal A, Mesa H, Knapp DJ, Kuskowski MA, Gupta P. Expression and phosphorylation of translation regulatory protein 4E-binding protein (BP)-1 in low-risk diffuse large B cell lymphoma. J Hematop. 2013;6:121-6.
117. Pourdehnad M, Truitt ML, Siddiqi IN, Ducker GS, Shokat KM, Ruggero D. Myc and mTOR converge on a common node in protein synthesis control that confers synthetic lethality in Myc-driven cancers. Proc Natl Acad Sci U S A. 2013;110:11988-93.
118. Mazan-Mamczarz K, Zhao XF, Dai B, Steinhardt JJ, Peroutka RJ, Berk KL et al. Down-Regulation of eIF4GII by miR-520c-3p Represses Diffuse Large B Cell Lymphoma Development. PLoS Genet. 2014;10:e1004105.
119. Horvilleur E, Sbarrato T, Hill K, Spriggs RV, Screen M, Goodrem PJ et al. A role for eukaryotic initiation factor 4B overexpression in the pathogenesis of diffuse large B-cell lymphoma. Leukemia. 2013;28:1092-102.
120. Kapadia B, Nanaji NM, Bhalla K, Bhandary B, Lapidus R, Beheshti A et al. Fatty Acid Synthase induced S6Kinase facilitates USP11-eIF4B complex formation for sustained oncogenic translation in DLBCL. Nat Commun. 2018;9:829.
121. Mallya S, Fitch BA, Lee JS, So L, Janes MR, Fruman DA. Resistance to mTOR Kinase Inhibitors in Lymphoma Cells Lacking 4EBP1. PLoS One. 2014;9:e88865.
122. Cencic R, Robert F, Galicia-Vázquez G, Malina A, Ravindar K, Somaiah R et al. Modifying chemotherapy response by targeted inhibition of eukaryotic initiation factor 4A. Blood Cancer J. 2013;3:e128.
123. Cencic R, Hall DR, Robert F, Du Y, Min J, Li L et al. Reversing chemoresistance by small molecule inhibition of the translation initiation complex eIF4F. Proc Natl Acad Sci U S A. 2011;108:1046-51.
124. Bordeleau M-E, Robert F, Gerard B, Lindqvist L, Chen SMH, Wendel H-G et al. Therapeutic suppression of translation initiation modulates chemosensitivity in a mouse lymphoma model. J Clin Invest. 2008;118:2651-60.

125. Schatz JH, Oricchio E, Wolfe AL, Jiang M, Linkov I, Maragulia J et al. Targeting cap-dependent translation blocks converging survival signals by AKT and PIM kinases in lymphoma. J Exp Med. 2011;208:1799-807.
126. Steinhardt JJ, Peroutka RJ, Mazan-Mamczarz K, Chen Q, Houng S, Robles C et al. Inhibiting CARD11 translation during BCR activation by targeting the eIF4A RNA helicase. Blood. 2014;124:3758-67.
127. Culjkovic-Kraljacic B, Fernando TM, Marullo R, Calvo-Vidal N, Verma A, Yang S et al. Combinatorial targeting of nuclear export and translation of RNA inhibits aggressive B-cell lymphomas. Blood. 2016;127:858-68.
128. Unterluggauer JJ, Prochazka K, Tomazic PV, Huber HJ, Seeboeck R, Fechter K et al. Expression profile of translation initiation factor eIF2B5 in diffuse large B-cell lymphoma and its correlation to clinical outcome. Blood Cancer J. 2018;8:79.
129. Campo E, Swerdlow SH, Harris NL, Pileri S, Stein H, Jaffe ES. The 2008 WHO classification of lymphoid neoplasms and beyond: evolving concepts and practical applications. Blood. 2011;117:5019-32.
130. Davies AJ, Rosenwald A, Wright G, Lee A, Last KW, Weisenburger DD et al. Transformation of follicular lymphoma to diffuse large B-cell lymphoma proceeds by distinct oncogenic mechanisms. Br J Haematol. 2007;136:286-93.
131. Vandesompele J, De Preter K, Pattyn F, Poppe B, Van Roy N, De Paepe A et al. Accurate normalization of real-time quantitative RT-PCR data by geometric averaging of multiple internal control genes. Genome Biol. 2002;3:research0034.1-.11.
132. Shipp MA, Ross KN, Tamayo P, Weng AP, Kutok JL, Aguiar RC et al. Diffuse large B-cell lymphoma outcome prediction by gene-expression profiling and supervised machine learning. Nat Med. 2002;8:68-74.
133. R Development Core Team. R: A language and environment for statistical computing [cited 1st July 2017]. Available from: https://www.r-project.org/.
134. Kwon OS, An S, Kim E, Yu J, Hong KY, Lee JS et al. An mRNA-specific tRNAi carrier eIF2A plays a pivotal role in cell proliferation under stress conditions: stress-resistant translation of c-Src mRNA is mediated by eIF2A. Nucleic Acids Res. 2017;45:296-310.

135. Gradi A, Imataka H, Svitkin YV, Rom E, Raught B, Morino S et al. A Novel Functional Human Eukaryotic Translation Initiation Factor 4G. Mol Cell Biol. 1998;18:334-42.
136. Liberman N, Gandin V, Svitkin YV, David M, Virgili G, Jaramillo M et al. DAP5 associates with eIF2β and eIF4AI to promote Internal Ribosome Entry Site driven translation. Nucleic Acids Res. 2015;43:3764-75.
137. Polymenis M, Aramayo R. Translate to divide: control of the cell cycle by protein synthesis. Microb Cell. 2015;2:94-104.
138. Hanahan D, Weinberg RA. Hallmarks of Cancer: The Next Generation. Cell. 2011;144:646-74.
139. Mao X, Green JM, Safer B, Lindsten T, Frederickson RM, Miyamoto S et al. Regulation of translation initiation factor gene expression during human T cell activation. J Biol Chem. 1992;267:20444-50.
140. Wang R, Geng J, Wang J-h, Chu X-y, Geng H-c, Chen L-b. Overexpression of eukaryotic initiation factor 4E (eIF4E) and its clinical significance in lung adenocarcinoma. Lung Cancer. 2009;66:237-44.
141. Jaiswal PK, Koul S, Shanmugam PST, Koul HK. Eukaryotic Translation Initiation Factor 4 Gamma 1 (eIF4G1) is upregulated during Prostate cancer progression and modulates cell growth and metastasis. Sci Rep. 2018;8:7459.
142. van der Knaap MS, van Berkel CGM, Herms J, van Coster R, Baethmann M, Naidu S et al. eIF2B-Related Disorders: Antenatal Onset and Involvement of Multiple Organs. Am J Hum Genet. 2003;73:1199-207.
143. Zoll WL, Horton LE, Komar AA, Hensold JO, Merrick WC. Characterization of mammalian eIF2A and identification of the yeast homolog. J Biol Chem. 2002;277:37079-87.
144. Rosenwald IB, Rhoads DB, Callanan LD, Isselbacher KJ, Schmidt EV. Increased expression of eukaryotic translation initiation factors eIF-4E and eIF-2 alpha in response to growth induction by c-myc. Proc Natl Acad Sci U S A. 1993;90:6175-8.
145. Kubica N, Crispino JL, Gallagher JW, Kimball SR, Jefferson LS. Activation of the mammalian target of rapamycin complex 1 is both necessary and sufficient to stimulate eukaryotic initiation factor 2Bε mRNA translation and protein synthesis. Int J Biochem Cell Biol. 2008;40:2522-33.

146. Sebestyen A, Sticz TB, Mark A, Hajdu M, Timar B, Nemes K et al. Activity and complexes of mTOR in diffuse large B-cell lymphomas-a tissue microarray study. Mod Pathol. 2012;25:1623-8.